ROADWAY SAFETY INSTITUTE

Human-centered solutions to advanced roadway safety

A Positioning and Mapping Methodology Using Bluetooth and Smartphone Technologies to Support Situation Awareness and Wayfinding for the Visually Impaired

Chen-Fu Liao

Department of Mechanical Engineering
University of Minnesota

Final Report

CTS 18-21

University of Minnesota Driven to Discover℠
The University of Akron
Illinois University of Illinois at Urbana-Champaign
Southern Illinois University Edwardsville
Western Michigan University

Technical Report Documentation Page

1. Report No.	2.	3. Recipients Accession No.
CTS 18-21		

4. Title and Subtitle	5. Report Date
A Positioning and Mapping Methodology Using Bluetooth and Smartphone Technologies to Support Situation Awareness and Wayfinding for the Visually Impaired	November 2018
	6.

7. Author(s)	8. Performing Organization Report No.
Chen-Fu Liao	

9. Performing Organization Name and Address	10. Project/Task/Work Unit No.
Department of Mechanical Engineering University of Minnesota 500 Pillsbury Drive SE Minneapolis, MN 55455	CTS#2015025
	11. Contract (C) or Grant (G) No. DTRT13-G-UTC35

12. Sponsoring Organization Name and Address	13. Type of Report and Period Covered
Roadway Safety Institute Center for Transportation Studies University of Minnesota 200 Transportation and Safety Building 511 Washington Ave. SE Minneapolis, MN 55455	Final Report
	14. Sponsoring Agency Code

15. Supplementary Notes

http://www.roadwaysafety.umn.edu/publications/

16. Abstract (Limit: 250 words)

People with vision impairment often face challenges while traveling in an unfamiliar environment largely due to uncertainty and insufficient accessible information. To improve mobility, accessibility, and the level of confidence the visually impaired experience in using the transportation system, it is important to remove information barriers that could potentially impede their mobility. A “condition aware” infrastructure using Bluetooth low-energy (BLE) technology was developed to provide up-to-date and correct audible information to users at the right location. A Multivariable Regression (MR) algorithm using the Singular Value Decomposition (SVD) technique was introduced to model the relationship between Bluetooth Received Signal Strength (RSS) and the actual ranging distance in an outdoor environment. This methodology reduced the environmental uncertainty and dynamic nature of RSS measurements in a Bluetooth network. The range output from the MR-SVD model was integrated with an extended Kalman filter to provide positioning and mapping solutions. Using 6 BLE beacons at an intersection in St. Paul, Minnesota, our approach achieved an average position accuracy of 2.5 m and 3.8 m in X and Y directions, respectively. A few statistical techniques were implemented and were able to successfully detect whether the location of one or multiple BLE beacons in a network changed based on Bluetooth RSS indications. With the self-monitoring network, information associated with each Bluetooth beacon can be provided to the visually impaired at the right location to support their wayfinding in a transportation network.

17. Document Analysis/Descriptors	18. Availability Statement
Bluetooth technology, Detection and identification systems, Navigation, Visually impaired persons	No restrictions. Document available from: National Technical Information Services, Alexandria, Virginia 22312

19. Security Class (this report)	20. Security Class (this page)	21. No. of Pages	22. Price
Unclassified	Unclassified	74	

A Positioning and Mapping Methodology Using Bluetooth and Smartphone Technologies to Support Situation Awareness and Wayfinding for the Visually Impaired

FINAL REPORT

Prepared by:

Chen-Fu Liao
Department of Mechanical Engineering
University of Minnesota

November 2018

Published by:

Roadway Safety Institute
Center for Transportation Studies
University of Minnesota
200 Transportation and Safety Building
511 Washington Ave. SE
Minneapolis, MN 55455

ACKNOWLEDGMENTS

The funding for this project was provided by the United States Department of Transportation's Office of the Assistant Secretary for Research and Technology for the Roadway Safety Institute, the University Transportation Center for USDOT Region 5 under the Moving Ahead for Progress in the 21st Century Act (MAP-21) federal transportation bill passed in 2012.

The author would like to thank the following individuals and organizations for their invaluable assistance in making this research possible.

- Sandeep Kumar and Charandeep Parisineti, former graduate students, Department of Computer Science Engineering, University of Minnesota (UMN)
- Professor Gordon Legge, Department of Psychology, UMN
- City of Saint Paul, MN
- Vision Loss Resources (VLR), Inc., Minneapolis, MN
- Minnesota Traffic Observatory (MTO), UMN
- Center for Transportation Studies (CTS), UMN

TABLE OF CONTENTS

CHAPTER 1: Introduction 1

1.1 Background 1

1.2 Objectives 2

1.3 Literature Review 2

1.3.1 Pedestrian Guidance Solutions 2

1.3.2 Accessible Pedestrian Signals (APS) 3

1.3.3 Work Zone Mobility for People with Disabilities 3

1.3.4 Auditory Messages for the Visually Impaired 4

1.3.5 Bluetooth Positioning using Received Signal Strength (RSS) 6

1.3.6 Measurement of Received Signal Strength Indication (RSSI) 7

1.3.7 Using Bluetooth RSS for Positioning 7

1.4 Report Organization 8

CHAPTER 2: Positioning and Mapping Using Bluetooth Low Energy Beacons 9

2.1 Introduction 9

2.2 Received Signal Strength Indication (RSSI) and Ranging 10

2.3 Singular Value Decomposition (SVD) Based RSSI Noise Reduction 13

2.3.1 SVD Calculation 14

2.3.2 SVD Reconstruction 14

2.3.3 Implementation 14

2.4 Enhanced Bluetooth Range Estimation Using RSSI from Multiple Beacons 15

2.4.1 RSSI and Distance Mapping 16

2.4.2 BLE Distance Estimation 17

2.5 Position Estimation Using Extended Kalman Filter (EKF) 18

CHAPTER 3: Detection of BLE Location and Network Configuration Changes 21

3.1 Statistical Process Control (SPC) 21
3.2 Wireless Signal Fingerprint 23
3.2.1 Jaccard Index 25
3.2.2 Normalized Weighted Signal Level Change 25
CHAPTER 4: Solar-Powered BLE System 27
4.1 Solar Charger System 27
4.2 Design of Solar Panel Mounting Fixture 28
CHAPTER 5: Experiment Results and Analysis 31
5.1 Program Bluetooth Low Energy (BLE) Beacons 31
5.2 Geospatial Database 35
5.3 RSSI Mapping and Positioning 36
5.3.1 Using 4 Beacons Powered by Coin Cell Battery 36
5.3.2 Using 6 Solar-Powered Beacons 38
5.4 CUSUM Analysis for Detecting BLE Location Changes 40
5.5 RSSI Fingerprint for BLE Network Configuration Changes 41
CHAPTER 6: Summary 44
6.1 System Benefits 45
6.2 System Limitations 46
REFERENCES 47
APPENDIX A Matric Differentiation
APPENDIX B Drawings of Solar Panel Mounting Assembly

LIST OF FIGURES

Figure 2.1 Smart beacons using Bluetooth 4.x technology. 10

Figure 2.2 BLE signal strength indication vs. distance (antenna facing vertically). 12

Figure 2.3 BLE signal strength indication vs. distance (antenna facing horizontally). 12

Figure 2.4 Raw Bluetooth RSSI measurements. 13

Figure 2.5 RSSI noise reduction using SVD (r=2). 15

Figure 2.6 RSSI noise reduction using SVD (r=1). 15

Figure 3.1 Illustration of normal inverse cumulative distribution function. 22

Figure 4.1 Solar charger system for a BLE beacon. 28

Figure 4.2 Solar panel mounting assembly. 28

Figure 4.3 Solar-powered BLE on a street light post 29

Figure 4.4 Installation of solar-powered BLE beacons in St. Paul, MN. 29

Figure 5.1 TI CC debugger and a BLE module. 31

Figure 5.2 GATT services running on each BLE module. 32

Figure 5.3 Image of a smartphone app for testing. 32

Figure 5.4 RSSI data collection and validation. 33

Figure 5.5 RSSI measurement vs. distance (indoor). 34

Figure 5.6 Average RSSI values of 4 Bluetooth devices by location 34

Figure 5.7 RSSI measurement and variation of 4 BLE beacons at location F and G. 34

Figure 5.8 RSSI vs distance relationship (outdoor). 35

Figure 5.9 Illustration of a geospatial database. 36

Figure 5.10 A simple Bluetooth network (background image from Google maps). 37

Figure 5.11 Sample RSSI measurements from 4 other BLE beacons at location G. 37

Figure 5.12 A Network of 6 BLE Beacons installed in downtown St. Paul, MN. 39

Figure 5.13 Sample RSSI measurements from 6 other BLE beacons at location D. 39

Figure 5.14 CUSUM and DI plots of a BLE moved away from its neighboring node. 40

Figure 5.15 Jaccard Index in normal condition. 41

Figure 5.16 Jaccard Index when BLE#21 was removed. 42

Figure 5.17 Jaccard Index when BLE#23 was removed. 42

Figure 5.18 NWSLC index in normal condition. 43

Figure 5.19 NWSLC index when BLE #23 was moved by 5 m. 43

Figure 5.20 NWSLC index when BLE #23 was totally moved. 43

LIST OF TABLES

Table 1.1 Versions of Bluetooth technology and data rate 7

Table 5.1 Comparison of absolute position error using different methodologies 38

Table 5.2 Comparison of absolute position error using more beacons 38

Table 5.3 CUSUM test results of moving BLE tags 40

LIST OF ABBREVIATIONS

ADA	Americans with Disabilities Act
ALF	Auditory Location Finder
AP	Access Point
APS	Accessible Pedestrian Signal
BLE	Bluetooth Low Energy
CDF	Cumulative Distribution Function
COTS	Commercially Off-The-Shelf
CTS	Center for Transportation Studies
CUSUM	Cumulative Sum
DOT	Department of Transportation
EDR	Extended Data Rate
EKF	Extended Kalman Filter
FHWA	Federal Highway Administration
GATT	Generic Attribute
GNSS	Global Navigation Satellite System
GPS	Global Positioning System
HAR	Highway Advisory Radio
HS	High Speed
IoT	Internet of Things
ISM	Industrial, Scientific and Medical
KF	Kalman Filter
KNN	K Nearest Neighbors
LCF	Logarithmic Curve Fitting
Li-ion	Lithium-ion
LiPo	Lithium-Ion Polymer
LOS	Line of Sight
LPF	Low Pass Filter
LSE	Least Square Estimation

MAC	Media Access Control
Mbps	Megabits per second
MR	Multivariable Regression
MTO	Minnesota Traffic Observatory
MUTCD	Manual on Uniform Traffic Control Devices
NEMA	National Electrical Manufacturers Association
NWSLC	Normalized Weighted Signal Level Change
O&M	Orientation and Mobility
RSI	Roadway Safety Institute
RSS	Received Signal Strength
RSSI	Received Signal Strength Indication
SD	Standard Deviation
SIG	Special Interest Group
SNR	Signal-to-Noise Ratio
SPC	Statistical Process Control
SVD	Singular Value Decomposition
SVM	Support Vector Machine
TAD	Travel Assistance Device
TI	Texas Instruments
TTC	Temporary Traffic Control
UMN	University of Minnesota
URTNA	Universal Real Time Navigational Assistance

EXECUTIVE SUMMARY

According to statistics from the 2015 National Health Interview Survey (NHIS) in the United States, more than 23.7 million American adults 18 years and older report experiencing significant vision loss. The number of individuals with vision impairment is expected to increase as the aging community continues to grow. The vast majority of people with vision impairment does not use any mobility device. Only a relatively small number of those with severe impairments uses a white cane or a guide dog as their primary tool for obstacle detection while traveling. Environmental cues, though not always reliable, are often used to support wayfinding and decision making by the visually impaired at various levels of navigation and situation awareness.

Due to differences in spatial perception as compared to sighted people, the visually impaired often encounter physical as well as information barriers along a trip. To improve their mobility, accessibility, and level of confidence in using the transportation system, it is important to remove not only the physical barriers but also the information barriers that could potentially impede their mobility and undermine safety.

The integrated Global Navigation Satellite System (GNSS) chipset on modern smartphones can usually provide reasonable positioning solutions in an open sky. However, in indoor or urban canyon conditions where GNSS receivers encounter significant multi-path interference from objects in the environment, positioning solutions are considerably worse. The positioning solutions from the smartphone become unreliable in GNSS-unfriendly or denied environments.

The latest Bluetooth technology (version 4.x or 5.0), Bluetooth Low-Energy (BLE), has considerably reduced power consumption as compared to the earlier versions of Bluetooth specifications. The low-cost BLE devices have enabled many applications using BLE tags and smartphone devices to locate or identify personal items, or alert owners when personal belongings are left behind.

We have developed a smartphone-based assistive system that incorporates a network of BLE beacons to provide location-specific traffic and navigational information for the visually impaired. The benefit of our approach is that the visually impaired need nothing more than a smartphone with text-to-speech capability to receive traffic information. In this report, we described a position sensing and a self-monitoring methodology. A network of BLE beacons was used to ensure that information provided to the visually impaired was up-to-date and at the correct location. We developed a methodology that uses the ability of a smartphone with Bluetooth to sense the proximity of Bluetooth modules and their ability to monitor each other.

However, Bluetooth wireless signals exhibit high variability in space and time, mostly because of the randomness of the radio signals, especially an issue in outdoor environments. In this research, we develop a methodology to incorporate the geometric characteristics of a network of BLE beacons to further reduce the effect of noise while using Received Signal Strength (RSS) for positioning. In addition, we modify the firmware of each BLE beacon that enables the forming of a self-monitoring network to ensure the integrity of network configuration, geometry, and information. The self-monitoring

functionality automatically reports network status, which reduces the maintenance required from public agencies. A crowdsourcing technique is also used to transmit information from a local BLE network to a cloud server through a user's smartphone network.

Furthermore, statistical methodologies were developed based on the Bluetooth RSS for positioning and self-monitoring. For mapping and positioning, we investigated several methodologies to find a more robust positioning solution that identified a user's relative location near an intersection. A Singular Value Decomposition (SVD) based Multivariable Regression (MR) algorithm was used to model the relationship between Received Signal Strength Indication (RSSI) and the actual ranging distance in an outdoor environment. This method reduced the environmental uncertainties and dynamic nature of RSSI measurements in a BLE network as compared to a simple Logarithmic Curve Fitting (LCF) model. The range output from the combined MR-SVD model was then integrated with an Extended Kalman Filter (EKF) technique to provide positioning solutions.

Due to the significant noise associated with the RSSI measurements, the LCF model has large position errors (7.3 and 9.5 m in X and Y axis, respectively). The MR-SVD and EKF combined model improves the position error by about 44% (to 4.1 and 5.4 m in X and Y axis, respectively) while using 4 battery-powered BLE beacons at an un-signalized intersection (Underwood St. & Judson Ave.) on the Minnesota State Fairgrounds. Additional experiments were later conducted at another un-signalized intersection (Washington St. & W 5th St.) in downtown St. Paul using 6 solar-powered BLE beacons. The results indicated further improvement of the position accuracy by about 30% to 2.5 and 3.8 m in X and Y direction, respectively.

Because of the low power characteristics of the BLE beacons, the RSS is subject to influences from many external parameters. The positioning errors of BLE-based solutions are affected by the environment (e.g., the busyness of traffic at an intersection) and the number of BLE beacons in a network. Adding more BLE beacons to the network or using wireless beacons with a higher Signal-to-Noise Ratio (SNR) could further improve the positioning accuracy.

For self-monitoring and maintaining the robustness and reliability of the BLE network, a Statistical Process Control (SPC) technique, called Cumulative Sum (CUSUM), is implemented to monitor whether the location of one or multiple BLE beacons in a network is changed based on the RSS measurements. In addition, two wireless signal fingerprinting techniques, namely, Jaccard and Normalized Weighted Signal Level Change (NWSLC) indices, are introduced to detect geometry changes of the BLE network. The results confirm that our methodologies are able to successfully detect the change of a BLE beacon when it is moved more than 3 to 6 m away or removed (e.g., due to vandalism or lost power) from a network.

In addition, a cloud-based geospatial database that contains the location and corresponding message of each BLE beacon is integrated with our smartphone app to provide situation awareness and corresponding navigation information to assist wayfinding for the visually impaired.

The intent of our assistive system is not to undermine the maintenance of skills and strategies that people with vision impairment have learned for navigation and wayfinding. Instead, the system aims to support their wayfinding capability, extend mobility and accessibility, and improve safety for the blind

and visually impaired. With the integration of the self-monitoring BLE network, our approach can locate the smartphone and ensure information associated with each BLE beacon provides the correct location to reliably support wayfinding for the visually impaired in a transportation network. The objective is to ensure that information provided to the visually impaired is up-to-date and at the correct location.

Although, our application was initially designed for people who are blind or visually impaired, the design can also benefit all users who prefer waypoint information guidance or require additional navigation information in an unfamiliar environment.

CHAPTER 1: INTRODUCTION

1.1 BACKGROUND

According to the fact sheet published by the World Health Organization (WHO) in 2017[1], there are about 253 million people who are visually impaired worldwide, and 36 million of them are blind. About 80% of the people who are blind or with vision impairment are aged 50 years and above. In the United States, 16.4 million American adults between the ages of 18 and 64 and 7.3 million American adults 65 years and older report experiencing significant vision loss[2]. As our community ages, more people will be at risk of vision impairment due to chronic eye diseases.

The blind and visually impaired usually travel on foot or use public transit as their primary mode of transportation to attend to their daily activities. Most of the people who are blind or visually impaired travel without any major barriers. However, some pedestrians who are blind could encounter physical and information barriers that limit their transportation accessibility and mobility.

According to statistics from the Federal Highway Administration (FHWA), each year approximately 17% of all work zone fatalities are pedestrians. If sighted pedestrians have this much difficulty, then imagine the problem that the visually impaired have. In addition to federal guidelines, MnDOT has invested a significant amount of effort to accommodate pedestrians, particularly those with disabilities, in temporary traffic control situations to ensure safe and effective movement.

After receiving orientation and mobility (O&M) training from O&M specialists, people with vision impairment can often travel long, complex, and novel distances independently. Some blind pedestrians use a white cane or a guide dog as a mobility tool for obstacle detection. However, neither of these mobility tools provides spatial awareness (such as work zone, traffic intersection, bus stops, skyway, or subway entrance) along with their path or guidance information to a destination at a distance. Travelers with vision impairment may have difficulty planning and feel anxious about attempting unfamiliar routes, often obtaining and closely following detailed turn-by-turn instructions to reach new destinations using their O&M skills. Physical and informational barriers thus discourage people who are blind or those with vision impairment from traveling in an unfamiliar environment.

The integrated Global Positioning System (GPS) chipset on cellular-enabled smartphones can usually provide reasonable positioning solution in the open sky. However, in indoor or urban canyon conditions where GPS receivers encounter significant multi-path interference from objects in the environment, positioning solutions are considerably worse. The positioning solutions from the smartphone become unreliable in GPS-unfriendly or denied environments.

---

[1] WHO, Vision impairment and blindness, Fact Sheet, Updated October 2017, http://www.who.int/mediacentre/factsheets/fs282/en/

[2] 2015 National Health Interview Survey (NHIS), https://www.cdc.gov/nchs/nhis/nhis_2015_data_release.htm

1.2 OBJECTIVES

To remove some of the information barriers to improved mobility of the visually impaired, this project focuses on enhancing safer travel for the visually impaired. The objectives of this proposal are to: (1) develop a "condition-aware, self-monitoring" infrastructure for supporting the location needs of the visually impaired in a GPS unfriendly environment, (2) determine what number of Bluetooth beacons are necessary to achieve a particular positioning accuracy for a Bluetooth Low-Energy (BLE) based positioning and mapping system, (3) use the generated local map as a reference and develop a smartphone-based interface to effectively convey geometry or navigational information (such as intersection, light rail crossing, etc.) to the visually impaired, and (4) interface the smartphone app with a geospatial database to identify a traveler's location and provide the corresponding audible messages via a text-to-speech interface on the phone to support wayfinding and situation awareness.

1.3 LITERATURE REVIEW

Though not always reliable, many environmental cues are available to support the decision making of people with vision impairment on various components of wayfinding. They often use auditory and limited visual information that they gather to make safe decisions while traveling in a transportation network. Although there are many aids (such as electronic, Braille map, etc.) to assist wayfinding in addition to cane or guide dog, blind people tend to use their cognitive map and spatial knowledge as primary guidance (Golledge & Garling, 2004). Giudice and Legge (2008) reviewed various technologies developed for blind navigation and concluded that no single technology can provide both indoor and outdoor navigation and guidance for the blind. It is critical to gain more insight from studying perception in order to have a clear understanding of the cognitive demands on the blind when they interpret information received by the sensory system.

For example, some blind pedestrians sometimes have difficulty crossing intersections at some locations due to the lack of information available to them about the traffic, geometry at intersections (Ponchillia et al., 2007; Barlow et al., 2005), and intersection types (signalized, un-signalized or roundabout). Guth et al. (2007) initially found that site-specific characteristics (for example, treatments such as rumble strips or speed countermeasures) appeared to have a greater impact on reducing the number of conflicts between pedestrians and vehicles than did a mobility device such as cane or guide dog. However, subsequent studies conducted by Bourquin et al. (2014, 2016, 2017 & 2018) found that a mobility cane had extremely high impact on drivers' yielding and the potential for significantly reducing conflicts.

1.3.1 Pedestrian Guidance Solutions

To provide signal information to blind users, Bohonos et al. (2008) demonstrated a Universal Real-Time Navigational Assistance (URTNA) system using Bluetooth beacons incorporated into a traffic controller to transmit signal timing to a user's cell phone. URTNA has proven that appropriate software can be developed, but a review of the literature yielded no further research in this area. Barbeau et al. (2010)

developed a Travel Assistance Device (TAD) using a GPS-enabled Smartphone to assist transit riders navigating the public transpiration system. The TAD prompts the rider in real-time with a recorded audio message, visual images, and vibration alerts when the rider should pull the stop request cord to exit the bus. It is especially helpful for those who are cognitively disabled. Ganz et al. (2011) used Radio-frequency identification (RFID) technology with a customized handheld device to support navigation for the blind in an unfamiliar indoor environment.

Some regions in Europe have begun to develop pedestrian navigation technology to assist the visually impaired or disabled, such as the Stockholm's e-Adept project (Josson et al., 2007; Dawidson, 2009; Johnni, 2009). Finland's NOPPA (Virtanen & Koshnen, 2004) project is designed to provide public transport passenger information and pedestrian guidance through a speech interface. The ASK-IT project (Bekiaris et al., 2007; Edwards, et al., 2007) partly funded by the European Commission under the 6th Framework Programme, uses personal profiling and web services to provide users with navigation, transportation and accessibility information. In France, the Mobiville project (Coldefy, 2009) aims to develop a real-time multimodal transportation information service and provide location-based navigation services for a pedestrian using GPS mobile phones.

Recently, Aira (2018) used smart glasses that relayed real-time video to a smartphone to guide vision-impaired travelers. But, it requires an off-site human assistant over the smartphone app to provide navigation information.

1.3.2 Accessible Pedestrian Signals (APS)

The Manual on Uniform Traffic Control Devices (MUTCD) recommends a rapid tick (percussive tome) for APS. A typical APS system generates percussive tome regularly to help the blind pedestrian locate the pushbutton. After an APS pushbutton is activated, the APS system announces an auditory message such as "Walk sign is ON" when the pedestrian signal display is in the "WALK" interval. Some APS systems can vocally count down the remaining time (in seconds) available to cross an intersection during the pedestrian "DON'T WALK" interval.

Previously, there were complaints about the noise generated by the earlier generation of APS from residents near the installations. The repeating tone adds 5 decibels of noise within 6 to 12 feet of the pushbutton. All modern APS have automatic volume control that automatically adjusts the sound volume based on the ambient traffic noise in the environment.

In the United States, an additional stub is often required for installing a pushbutton station. Ongoing maintenance and Braille verification require additional effort. Liao (2013) developed a mobile accessible pedestrian signal system that allows a user to obtain intersection geometry and traffic signal information from a smartphone.

1.3.3 Work Zone Mobility for People with Disabilities

According to statistics from the Federal Highway Administration (FHWA), each year approximately 17% of all work zone fatalities are pedestrians. Since the Americans with Disabilities Act (ADA) was enacted in

1990, there has been growing emphasis from both federal and local transportation agencies to provide safe pedestrian access in and around work zones. The ADA requires that pedestrians with disabilities be accommodated in completed facilities as well as during times of construction.

The MUTCD published by the FHWA and the Minnesota MUTCD (part 6) provides specific guidelines for Temporary Traffic Control (TTC) in work zones and outline specific requirements to accommodate pedestrians with disabilities (MN MUTCD, 2011). One of the requirements is, for example, to provide audible information for the visually impaired. Ullman & Trout (2009) emphasized the importance of clear audible messages and spatial message elements that are critical in guiding visually impaired pedestrians along a temporary route and supporting navigation in a less familiar environment.

A few pedestrian audible devices with pushbutton or motion-activated options are commercially available. For example, Empco-Lite and the ADA SpeakMaster™ from MDI Traffic Control Products use pre-recorded messages at selected locations around a work zone to inform approaching pedestrians about the construction and provide specific routing information.

These audible warning devices are usually placed at a specified distance before the actual sidewalk closure. As the pedestrian approaches, he/she hears a unique locator tone that indicates more information is available. The locator tone can be programmed to play continuously or be activated by an optional motion sensor. After locating the pushbutton, the pedestrian activates the voice module to hear navigation instructions to safely pass through the temporary pedestrian access route.

One concern about these audible systems is the consistency of information elements in a pre-recorded message and its clarity in an outdoor environment (Ullman & Trout, 2009). In addition, information overload could be another concern as most people may have difficulties in memorizing long verbal messages accurately. Transportation engineers and practitioners often face challenges between verbosity and efficiency of auditory messages. Liao (2013, 2014) recently incorporated work zone routing information into the previously developed smartphone application to alert pedestrians as they approach a work zone.

1.3.4 Auditory Messages for the Visually Impaired

The MUTCD clearly states that auditory messages should be used in and around work zones for people with disabilities; however, there is limited guidance available on auditory message structure and elements. Currently, there is insufficient guidance on how the audible message should be formatted to support wayfinding for the visually impaired around work zones.

For example, Bentzen et al. (2002) recommended a speech message structure and wording for APS. Hine et al. (2000) developed an Auditory Location Finder (ALF) that involved auditory message content, structure, route choice, orientation, landmarks, and clues. Giudice et al. (2007) studied spatial learning and navigation using dynamically updated verbal messages and employed a geometric-based display consisting of three verbal modes (local, maplet, and global). They concluded that dynamically updated verbal descriptions are an effective medium to describe environmental relations and support spatial learning in unfamiliar environments.

In addition, Ullman & Trout (2009) explored different audio message elements and investigated how the guidance and warning messages were being understood by the visually impaired. They identified the number of units of information in each message based on Highway Advisory Radio (HAR) message guidance. They concluded that it is important to (1) design a clear, simple and concise message, and (2) include an initial turning or crossing instruction and travel distance (preferably using blocks for long distance and feet for a shorter distance) as critical message elements for navigating an alternate route. They also indicated that there is still a concern about information overload.

Gaunet and Briffault (2005, 2006) studied guidance instructions and spatial information through navigational experiments in both simple structured and complex unstructured urban areas. They used six categories of guidance functions to structure linguistic forms for synthesizing the perceptual and environmental information. They suggested that the detail level of description and precision of localization must be improved to provide guidance in complex urban environments. The information guidance functions consist of Location and Orientation (LO) and Goal Location (GL). The instruction guidance functions include Orientation (O), Crossing (C), Route Ending (RE), and Progress (P) (Gaunet and Briffault, 2005).

Havik et al. (2011) recommended including distance information to the next information point and more landmarks or information points in electronic travel aids in assisting wayfinding for visually impaired users. An auditory interface is simple, straightforward, and effective in guiding users along both simple and complex paths (Wilson et al., 2007).

The above is fine and good if the visually impaired can trust that the information provided is valid and robust. We need a “condition aware” infrastructure, i.e., a system that can self-monitor and make sure that the information is up to date.

The low-cost BLE devices have enabled many applications using BLE tags and smartphone devices to locate or identify a personal item, or alert owners when personal belongings are left behind. Some applications use crowdsourcing to help retrieve lost items when the items are out of the owners’ Bluetooth communication range. However, these BLE tags, primarily designed to be detected or discovered, do not communicate with each other.

We propose a standalone Bluetooth smart system (called BLE-master) that integrates a commercial off-the-shelf BLE module operating in dual modes (master/slave) with necessary interface elements to sense other BLE-master devices within its range of communication. A positioning and mapping algorithm will be developed to create a local map of an unfamiliar or hazardous environments (such as a complicated intersection). The BLE-master units will remember and check the other BLE-master devices in their communication range to ensure the integrity of the local map and to provide correct positioning information in GPS-denied environments.

A geospatial database that contains the location and corresponding message of each BLE device will be integrated with a smartphone app to provide reliable situation awareness and corresponding navigation information to assist wayfinding for the visually impaired. The mapping methodology ensures correct

audible information (such as signal timing and intersection geometry) is provided to users at the right location.

1.3.5 Bluetooth Positioning using Received Signal Strength (RSS)

GPS has been widely used for outdoor navigation. However, due to the significant loss of satellite signal reception inside buildings, it is difficult to acquire reliable positioning using the GPS technology.

Many different approaches, such as Wi-Fi, infrared light, ultrasound, Bluetooth, etc., are used for positioning and location sensing. Wi-Fi devices usually consume more power than Bluetooth devices. In recent years, the Bluetooth technology has increasingly been used for communication among consumer electronics, particularly mobile devices such as smartphone/tablet devices, due to its low cost, low power consumption, and ease of integration characteristics. Bluetooth technology is often used to transfer information between two or more devices that are near each other in relatively low-bandwidth situations. Bluetooth operates in the range of 2400–2483.5 MHz under the Industrial, Scientific and Medical (ISM) 2.4 GHz short-range radio frequency band. Bluetooth uses frequency-hopping technology. Transmitted data are divided into packets and each packet is transmitted on one of the 79 designated Bluetooth channels (Bluetooth SIG).

Many studies in the literature investigated the functional capability and signal characteristics of earlier versions of Bluetooth devices for positioning and location sensing (Kotanen et al., 2003; Castaño et al., 2004; Bandara et al., 2004; Almaula & Cheng, 2007; Altini et al., 2010; Diaz et al., 2010, Pei et al., 2010; Oliveira et al., 2012; Wang et al., 2013; Oguejiofor et al., 2013). Hossain & Soh (2007) investigated four Bluetooth signal parameters (connection-based Received Signal Strength Indication (RSSI), link quality, transmit power level, and inquiry-based RSSI) for Bluetooth localization and positioning. The inquiry-based RSSI does not require an active connection between Bluetooth devices. It monitors the received power level of inquiry responses from a nearby Bluetooth device and infers the corresponding RSSI value. Hossain & Soh (2007) confirmed that inquiry-based RSSI provide better measurements than the connection-based RSSI and other parameters.

Table 1 lists the Bluetooth versions and their corresponding maximum date rate and typical ranges of communication. The Bluetooth 3.0 High Speed (HS) specification was introduced in 2009 with a data transfer speed up to 24 Mbit/s. BLE 4.0 specification was introduced in 2010. The high-speed and low-energy protocols have enabled a plethora of applications for Internet of Things (IoT). BLE 4.1 and 4.2 were later released in 2013 and 2014, respectively. Unveiled in 2016, Bluetooth 5 offers options including 2X the speed, or up to 4X the range, and 8X the data broadcasting capacity.

Table 1.1 Versions of Bluetooth technology and data rate

Version	Maximum Data Rate	Range
1.2	1 Mbit/s	Class 1: 100 meters (328 feet) Class 2: 10 meters (33 feet) Class 3: 1 meters (3 feet) Class 4: 0.5 meters (1.6 feet)
2.0 + EDR	3 Mbit/s	
3.0 + HS	24 Mbit/s	
4.x (BLE)	24 Mbit/s (throughput 1 Mbps)	Up to 100 meters or 328 feet
5.0 (BLE)	48 Mbit/s (throughput 2 Mbps)	Up to 300 meters or 985 feet

1.3.6 Measurement of Received Signal Strength Indication (RSSI)

The latest Bluetooth technology (version 4.0), Bluetooth Low Energy (BLE) or Bluetooth Smart, has considerably reduced power consumption as compared to earlier versions. The low-cost BLE devices have enabled many applications using BLE tags and smartphone devices to locate or identify personal items, or alert owners when personal belongings are left behind. When the smartphone app receives the wireless signal from a BLE tag, it also receives a RSSI value with that broadcasted message. The RSSI is used to evaluate the distance from the tag. Some applications use crowdsourcing to help retrieve lost items when the items are out of the owners' Bluetooth communication range (50-70 meters based on the line of sight).

Kikawa et al. (2010) developed a presence detection methodology using the RSSI of a Bluetooth device and a judgment time threshold. Liao (2013 & 2014) developed a smartphone app, in connection with Bluetooth (ver.2.1+EDR) beacons placed at key decision points around a work zone to provide situation awareness along with routing or bypassing information to the visually impaired. A geospatial database of the locations of the Bluetooth beacons was developed to allow the smartphone app to query audible message associated with discovered Bluetooth beacons.

Faheem et al. (2010) developed an RSSI-based distance estimation technique by optimizing the standard deviation (SD) of the RSSI and the packet of loss information along with the curve parameters for minimal distance error.

1.3.7 Using Bluetooth RSS for Positioning

Bandara et al. (2004) evaluated the Bluetooth positioning model using RSSI and proposed a multi-antenna Bluetooth access point that supports variable attenuators to reduce the error rate. The test obtained 2 meters of error in a 4.5 m by 5.5 m area with 4 antennas. Sheng & Pollard (2006) used RSSI and a radio signal propagation model to estimate the distance between a pair of Bluetooth transmitters and receivers. However, high density of Bluetooth infrastructure is required to achieve accurate positioning.

Triangulation methodology and signal propagation modeling were studied for indoor and outdoor positioning and sensing applications (Almaula & Cheng, 2006; Oguejiofor et al., 2010; and Wang et al., 2013).

Subhan et al. (2011) used a gradient filter and a signal propagation model to improve the positioning accuracy to 2.67 m in Bluetooth networks. Zhang et al. (2013) studied three fingerprinting-based Bluetooth positioning algorithms, k nearest neighbor (kNN), support vector machine (SVM), and neural networks. They evaluated the accuracy and precision of Bluetooth positioning using an Android mobile phone and 5 other Bluetooth beacons in a lab office. They concluded the kNN regression method outperforms the other two algorithms studied.

Fingerprinting is a common technique for indoor positioning. The fingerprinting technique usually includes two phases: data training and real-time location determination. Pei et al. (2010) approximated the Bluetooth signal strength distribution using the Weibull probability distribution function (Sagias and Karagiannidis, 2005) with limited RSSI samples in a training phase. A histogram maximization likelihood position estimation based on Bayesian theory (Youssef et al., 2003; Roos et al., 2002) was then used in positioning phase. The results indicated that the fingerprinting solution using the Weibull probability distribution performed better than the occurrence-based approach. But, the fingerprinting approach required a dynamic reference model of RSSI for each location in order to compare all measured signals to determine the position in an outdoor environment, e.g., a traffic intersection.

Wang et al. (2010 & 2013) explored the relations between distance and signal strength of Bluetooth devices using least square estimation (LSE) and trilateration. The results indicated that the LSE method can closely estimate the distance between Bluetooth devices based on the received signal strength (RSS) in an open space. However, RSS is dependent on its terrain and transmission obstacles in the environment. Our approach incorporated a methodology that considers the RSS characteristics in a local network of BLE beacons to better model the actual distance between BLE sensors and RSS in a dynamically changing environment.

1.4 REPORT ORGANIZATION

The rest of this report is organized as follows. A Singular Value Decomposition (SVD) based Multivariable Regression (MR) algorithm for positioning and mapping is presented in Chapter 2. A statistical process control and two wireless signal fingerprinting techniques for detecting location and geometry changes of a BLE network are discussed in Chapter 3. A solar power charger design and a mounting fixture for the BLE beacons were developed and presented in Chapter 4. Analysis results using the RSS measurements from Bluetooth Low Energy (BLE) beacons are discussed in Chapter 5. Finally, a summary of this project is included in Chapter 6.

CHAPTER 2: POSITIONING AND MAPPING USING BLUETOOTH LOW ENERGY BEACONS

2.1 INTRODUCTION

Bluetooth technology has been used in recent year as an inexpensive and reliable way to collect travel time information on roadways (Martchouk et al., 2011). Anonymous travel time monitoring is performed by matching the Media Access Control (MAC) addresses of Bluetooth devices embedded on cell phones or GPS navigation devices. Bluetooth technology does not require line of sight (LOS). However, its signal attenuation may be influenced by physical obstacles.

The latest Bluetooth technology (4.x and 5.0), Bluetooth Low Energy (BLE) or Bluetooth Smart, has considerably reduced power consumption as compared to earlier versions. Low-cost BLE devices have enabled many applications using BLE tags and smartphone devices to locate or identify personal items, or alert owners when personal belongings are left behind. The Received Signal Strength Indication (RSSI) of Bluetooth can be used to estimate the distance between smart devices. The newer generation of smartphones on the market is now equipped with BLE technology. For example, iBeacon from Apple uses BLE technology to identify locations which trigger an action on the iPhone. According to an article "*Mobile Telephony Market*", the Bluetooth Special Interest Group (SIG) indicated that more than 90% of Bluetooth-enabled smartphones will support the low energy standard by 2018.

The GPS satellite positioning system provides relatively accurate user location in an open space. However, in urban canyons or indoor environments, the position solution is unavailable or degraded due to signal strength, reflections, multipath, and other factors. The purpose of using Bluetooth devices as smart beacons is to identify a pedestrian's location more accurately and reliably at a decision location or a point of interest (for example, corner of an intersection, bus stop, entrance of a building, etc.).

A Bluetooth beacon operating in a receiving mode can be installed at decision points to serve as a geo-reference IDs which can be detected by the smartphone application to identify the user's location. When operating in the receiving mode, the Bluetooth beacon consumes minimal power ranging from 15 to 50 milliwatts (mW). The Bluetooth beacon can be either connected to the battery of a barricade flasher or operated using a very small solar panel.

New development of low power Bluetooth 4.x technology, as shown in Figure 2.1, allows Bluetooth beacons to operate on a single coin cell battery. The low power consumption feature of Bluetooth devices running in discovery mode for the proposed work zone application could extend the battery life significantly. The smaller package size (similar to the size of a US dollar coin) will make it even easier to deploy by attaching the Bluetooth beacons on barricades, traffic cones, or flashers in a work zone.

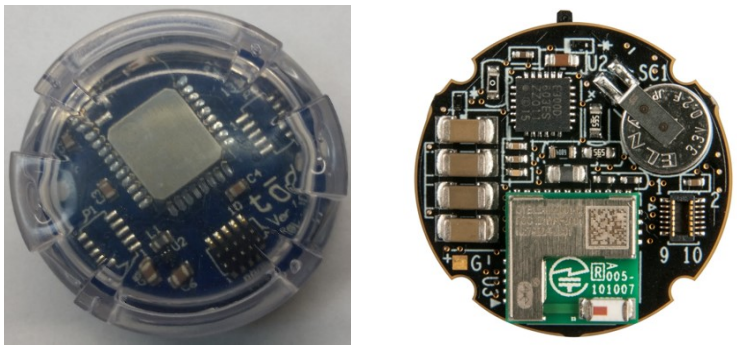

Figure 2.1 Smart beacons using Bluetooth 4.x technology.

2.2 RECEIVED SIGNAL STRENGTH INDICATION (RSSI) AND RANGING

Many indoor localization methodologies using Bluetooth technology have been studied (He et al., 2017; Kalbandhe & Patil, 2016; Zhuang et al., 2016; Chen et al., 2016; Yoon et al., 2015; Palumbo et al., 2015; Rida et al., 2015; Faragher & Harle, 2014; Mautz, 2012; Shi, 2012; Fink & Beikirch, 2011; Zhao et al., 2011; Chen et al., 2010; Pei et al., 2010; Liu et al., 2010). For example, He et al. (2017) investigated the number of beacons required for unambiguous positioning. Chen et al. (2016) developed an indoor methodology using inertial sensors on a smartphone with the aid of positioning corrections from iBeacons[3]. Their results indicated that the placement of iBeacons will greatly affect the localization accuracy. The iBeacon is a protocol developed by Apple[4]. It is based on Bluetooth low energy proximity sensing.

Raghavan et al. (2010) reported a positioning error less than 1 meter using class 2 Bluetooth devices. Subhan et al. (2011 & 2013) used fingerprinting, lateration and Kalman filter based approaches to estimate an indoor location of a Bluetooth network. Their results indicated that the average indoor position error ranges from 1 to 2 meters.

Researchers have used Kalman filters (Zhuang et al., 2016; Subhan et al., 2013; Ozer & John, 2016), fingerprinting (Faragher & Harle, 2014) and lateration (Zhuang et al., 2016; Zhu et al., 2014; Subhan et al., 2013) based approaches to estimate an indoor location of a Bluetooth network. The fingerprint-based positioning approach (Faragher & Harle, 2015; Davidson & Piché, 2017) typically divides the area into a grid pattern and requires a survey of signal fingerprints performed in advance which serve as a reference for each grid cell. The observed wireless signal fingerprint at a user's location is then compared to the reference in order to determine the user's location at the grid level. This approach is not suitable for outdoor environments where wireless signal patterns may change dynamically.

Dong & Dargie (2012) investigated the reliability of RSSI for indoor localization. They calibrated and mapped RSSI to distance through a series of experiments. They concluded that the RSSI values give a

[3] iBeacon, https://en.wikipedia.org/wiki/IBeacon
[4] Apple, https://developer.apple.com/ibeacon/

considerable fluctuation in a mobile scenario and thus are not reliable for the indoor sensor localization. Jung et al. (2013) used a simple low-pass filter (LPF) to reduce RSSI noises. However, the LPF is not effective. Subhan et al. (2015) presented an extended gradient filter and predictor to address the communication holes of the RSSI caused by signal attenuation, signal loss, multi-path effects. Their results using both simulated and actual data indicated that the extended gradient filter and predictor methodology performs better than the gradient filter and also works better than Kalman filter and Kalman smoother. Faragher and Harle (2014) investigated the positioning accuracy of Bluetooth Low Energy devices in advertising mode for fingerprint-based indoor position schemes. They concluded that the positioning accuracy increases with the number of beacons per fingerprint, up to 6–8 beacons.

Ideally, an RSSI value can be converted to receive power level if both upper and lower power thresholds are known. A simple log-distance model (Kotanen, et al., 2003) can be described as follows.

$$P_{RX} = P_{TX} + G_{TX} + G_{RX} + 20\log(\lambda) - 20\log(4\pi) - 10nlog(d) - X_a \quad (2\text{-}1)$$

Where,

P_{TX} and P_{RX} are the power level of the transmitter and receiver,

G_{TX} and G_{RX} are the antenna gain of the transmitter and receiver,

λ is the wavelength (about 0.12 m for 2.441 GHz Bluetooth channels),

d is the distance between the transmitter and the receiver,

n is a factor that describes the influence of environmental obstacles, and

X_a is the noise

Or, the received Bluetooth power level can be expressed in a simplified model (Zhu et al., 2014) based on the radio propagation model as shown in Eq. (2-2) which describes the relationship between the signal received and distance. The received power decreases logarithmically with distance, where $P(d)$ is the received signal power, $P(d_0)$ is the signal strength at a reference point d_0, and γ is the path loss exponent (typically between 1 and 4).

$$P(d) = P(d_0) - 10\gamma\log\left(\frac{d}{d_0}\right) \quad (2\text{-}2)$$

We evaluated the RSSI of the Bluetooth Low Energy (BLE) devices[5] mounted in a different orientation in an outdoor environment. Figure 2.2 and 2.3 display the relationship if RSSI vs. distance of a BLE module mounted vertically and horizontally on a lamp post. The RSSI values have a large range of variation at a given distance. The median and average RSSI values are relatively close to each other. The RSSI and

[5] Bluegiga BLE112 Bluetooth® Smart Module, https://www.silabs.com/products/wireless/bluetooth/bluetooth-low-energy-modules/ble112-bluetooth-smart-module

distance relationship was modeled using a logarithmic least square fitting technique with the R-square value of 0.83 and 0.84, respectively.

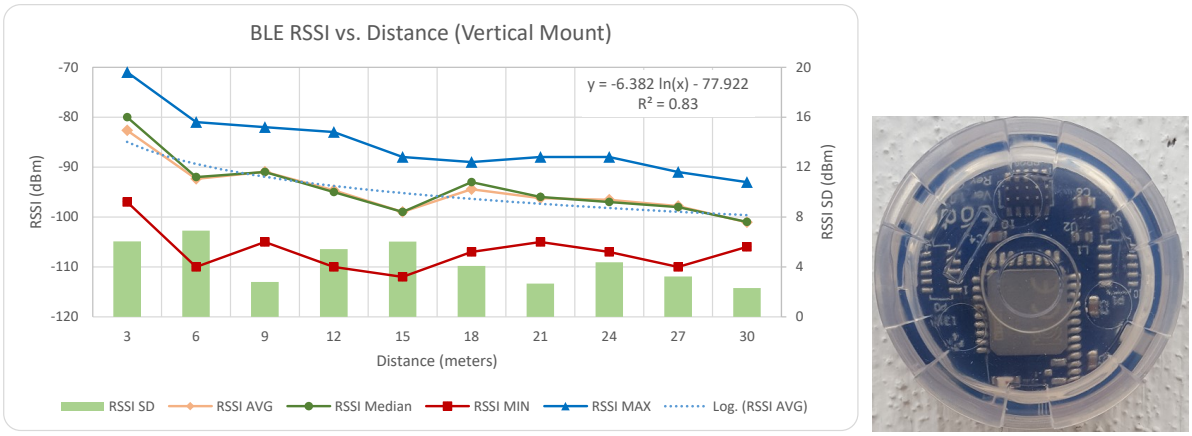

Figure 2.2 BLE signal strength indication vs. distance (antenna facing vertically).

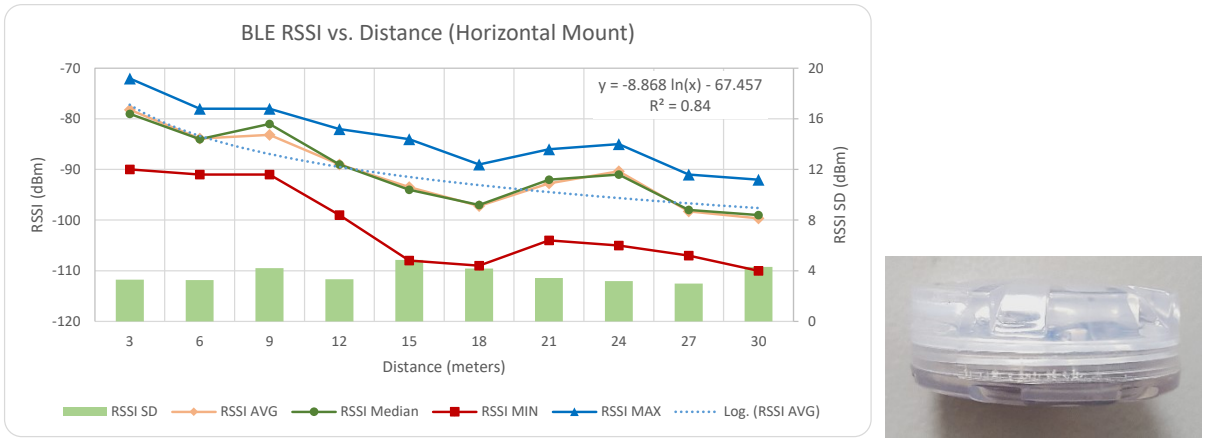

Figure 2.3 BLE signal strength indication vs. distance (antenna facing horizontally).

As our results indicated (Figure 2.3), the Bluetooth RSSI values exhibit high variability in space and time. Suárez et al. (2010) compared the performance of a Kalman filter and a gradient filter in handling the communication holes of RSSI values. We used a Singular Value Decomposition (SVD) approach to reduce noises of RSSI measurements (Fan & Lin, 2008).

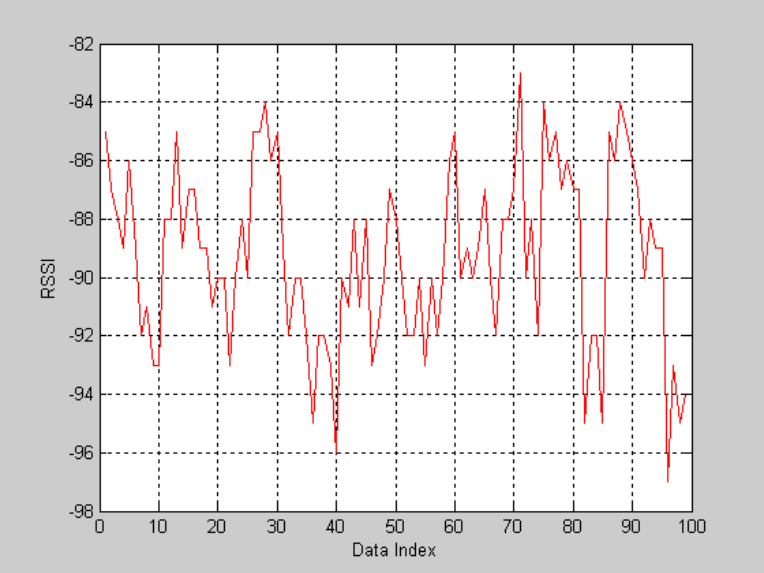

Figure 2.4 Raw Bluetooth RSSI measurements.

2.3 SINGULAR VALUE DECOMPOSITION (SVD) BASED RSSI NOISE REDUCTION

The RSSI measurements can be expressed as a vector in a D-dimensional space with noise and pure signal lying in orthogonal subspaces. A Hankel matrix is constructed for the RSSI measurements for altering its singular spectrum. The high energy components are supposed to contain the pure signal, whereas the low energy components are supposed to contain only noise. The RSSI measurements y consists of the pure signal x and the noise n as:

$$y(i) = x(i) + n(i) \tag{2-3}$$

Where i representes the index of BLE beacons, $y(i)$ and $n(i)$ represent the RSSI values and environment noise from the i-th BLE beacon, respectively.

Therefore, we create overlapping frames of D samples of the RSSI measurements, $Y = [y(0), y(1), y(2), \ldots, y(D-1)]^T$. A Hankel-form matrix, H_Y, is expressed as,

$$H_Y = \begin{bmatrix} y(0) & y(1) & \ldots & y(M-1) \\ y(1) & y(2) & \ldots & y(M) \\ \vdots & \vdots & \ddots & \vdots \\ y(K-1) & y(K) & \ldots & y(D-1) \end{bmatrix} \tag{2-4}$$

The dimension H_Y is $K \times M$, where $K \geq M, and\ M + K = T + 1$.

According to the assumption of additive noise, we can also write,

$$Y = X + N \tag{2-5}$$

Where Y, X, and N are the raw RSSI measurement, pure RSSI signal and noise vectors, respectively.

2.3.1 SVD Calculation

Using the SVD technique, the matrix H_Y can be decomposed and expressed as,

$$H_Y = U\,\Sigma\,V^T \tag{2-6}$$

Where,

$U \in \mathcal{R}\,(K \times K)$ is the orthonormal left singular vector,

$V \in \mathcal{R}\,(M \times M)$ is the orthonormal right singular vector, and

$\Sigma = \text{diag}\,(c_1, c_2, \ldots, c_p)$, $c_1, c_2, \ldots, c_p$ are the singular values of the noisy matrix, H_Y.

$c_1 \geq c_2 \ldots \geq c_p \geq 0$ and $p = \min(K, M)$.

2.3.2 SVD Reconstruction

The largest singular components in equation (2-6) capture almost only signal information whereas the smallest ones contain almost only noises. The noise reduction can be obtained by adopting a diagonal weighting matrix W to equation (2-6).

$$H_{\hat{X}} = U\,(W\Sigma)\,V^T \tag{2-7}$$

Matrix $H_{\hat{X}}$ is no longer in Hankel form. However, the non-diagonal components of $H_{\hat{X}}$ can be averaged to extract the imparoived signal $\bar{X} = [\hat{x}(0), \hat{x}(1), \hat{x}(2), \ldots, \hat{x}(D-1)]^T$.

A Least Square (LS) estimation or rank reduction approach is applied to select the weighting matrix W. We assume the pure RSSI signal X consists of r complex components such that the rank of $H_{\hat{X}}$ is r. The LS estimates of H_Y is obtained by setting the $M - r$ smallest eigenvalues to zero.

$$H_{Y,r} = [U_r \quad U_{M-r}] \begin{bmatrix} \Sigma_r & 0 \\ 0 & 0 \end{bmatrix} \begin{bmatrix} V_r^T \\ V_{M-r}^T \end{bmatrix} \tag{2-8}$$

Where Σ_r contains the r largest singular values, and $H_{Y,r}$ is the best rank-r estimation of H_Y.

2.3.3 Implementation

The SVD based RSSI noise reduction discussed in section 2.3.1 & 2.3.2 were implemented and tested using the raw RSSI signal as illustrated in Figure 2.4. Figure 2.5 displays the results of the filtered RSSI signal using LS estimation with rank $r = 2$. The resulting singular values found in this case are $c_1 = 4{,}473, c_2 = 49$. We further reduce the rank to 1 because the two largest singular values differ by two orders of magnitude. Figure 2.6 shows the results of the filtered RSSI signal using LS estimation with rank $r = 1$.

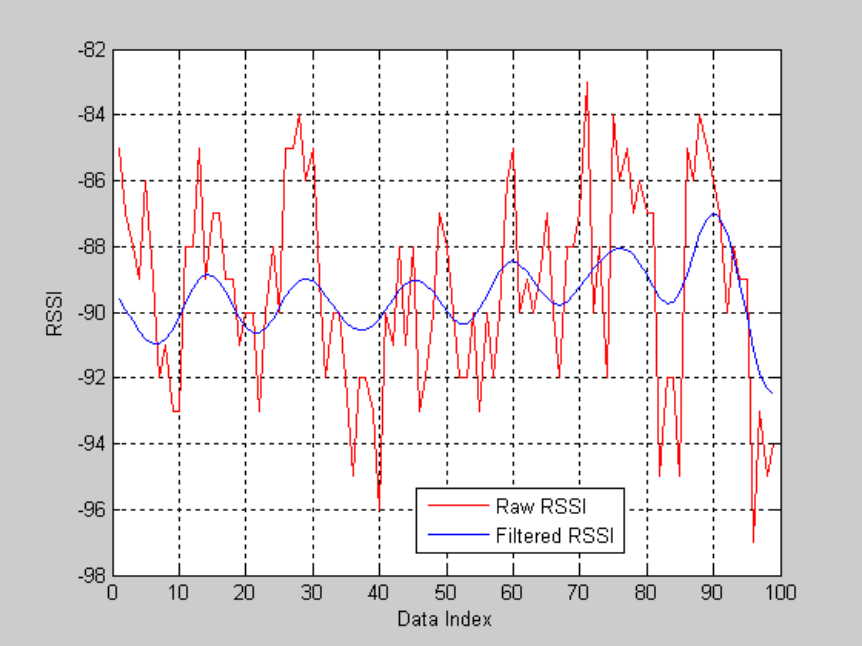

Figure 2.5 RSSI noise reduction using SVD (r=2).

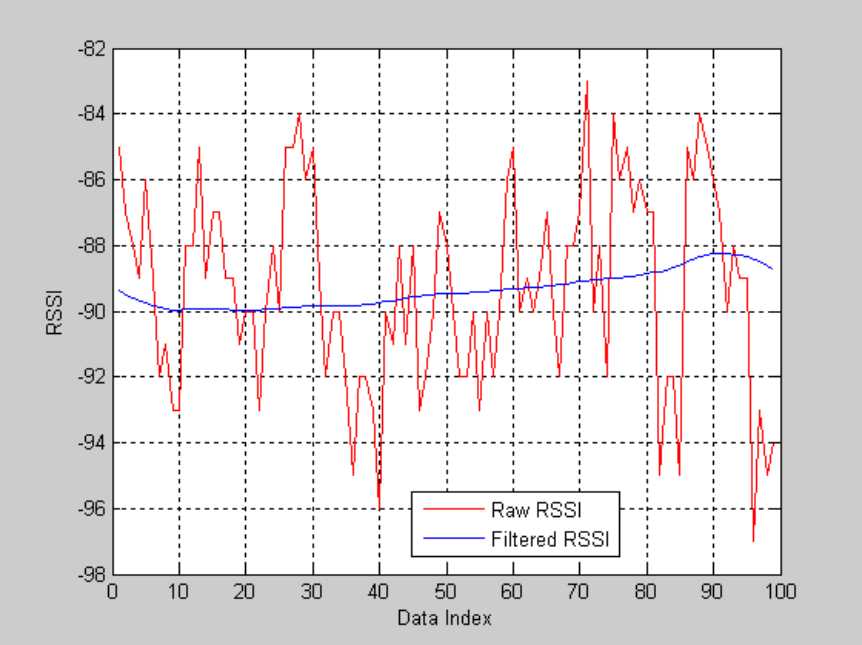

Figure 2.6 RSSI noise reduction using SVD (r=1).

2.4 ENHANCED BLUETOOTH RANGE ESTIMATION USING RSSI FROM MULTIPLE BEACONS

Fan et al. (2015) proposed an SVD-based Multivariable Regression (MR) approach by including signal strength from multiple Access Points (AP) in a cellular network for mobile device localization. Due to the environmental dynamics, nature of Bluetooth wireless medium and the uncertainties in the power-distance model as described in section 2.3, we adopted the approach proposed by Fan et al. (2015) for a

Bluetooth Low Energy (BLE) network. The goal is to create a mapping between RSSI and distance using the MR-based approach in real-time to better characterize the RSSI-distance relationship at an intersection. Our approach is used to better estimate the distances between a smartphone and BLE beacons based a local mapping of the received Bluetooth signals. The estimated distances between a smartphone and BLE beacons are then incorporated into an Extended Kalman Filter (EKF), which will be described in the following section, for positioning estimation.

2.4.1 RSSI and Distance Mapping

A Multivariable Regression (MR) model is selected to map the distance from a BLE to all the other BLE beacons to be described by a weighted combination of RSSI values from all BLE beacons. The MR model is expressed as,

$$\log(d_i) = S_i W_i + \varepsilon_i \tag{2-9}$$

Where,

$D_i = [d_1, d_2, \dots, d_n]$ is n distance matrix from i-th BLE to n-th BLE beacons,

$d_i = [d_{in}^1, d_{in}^2, \dots, d_{in}^m]^T$ is m distance values from i-th to n-th BLE beacons,

S_i refers to the input variables of the i-th BLE,

$W_i = [w_0, w_1, \dots, w_n]^T$ is the weighting matrix, and

ε_i is an error term.

For m RSSI records received by i-th BLE, the corresponding d_i and S_i matrices are expressed as the following, respectively.

$$D_i = \begin{bmatrix} d_{i1}^1 & d_{i2}^1 & \dots & d_{in}^1 \\ d_{i1}^2 & d_{i2}^2 & \dots & d_{in}^2 \\ \vdots & \vdots & \ddots & \vdots \\ d_{i1}^m & d_{i2}^m & \dots & d_{in}^m \end{bmatrix} \tag{2-10}$$

$$S_i = \begin{bmatrix} 1 & s_{i1}^1 & \dots & s_{in}^1 \\ 1 & s_{i1}^2 & \dots & s_{in}^2 \\ \vdots & \vdots & \ddots & \vdots \\ 1 & s_{i1}^m & \dots & s_{in}^m \end{bmatrix} \tag{2-11}$$

Where,

d_{in}^m refers to the m-th distance measurement between the i-th and the n-th BLE, and

s_{in}^m is the m-th RSSI value received by the i-th BLE from the n-th BLE beacon.

The matrix D_i $(m \times n)$ contains m regress outputs, indicating m estimated distances from multiple RSSI values. The matrix S_i is a $m \times (n+1)$ matrix. The weighting W_i represents a regression by which the RSSI values are combined to determine distance. The weighting W_i can be obtained by using a linear MR approach to minimize the sum of squared residuals (SSE) which is defined as,

$$SSE_i = \varepsilon_i^T \varepsilon_i = [\log(d_i) - S_i W_i]^T \, [\log(d_i) - S_i W_i] \tag{2-12}$$

To minimize SSE_i, we can take the derivative of SSE_i with respect to W_i,

$$\frac{\partial(SSE_i)}{\partial(W_i)} = 0 \tag{2-13}$$

Therefore,

$$\partial(-\log(d_i)^T S_i W_i - {W_i}^T {S_i}^T \log(d_i) + {W_i}^T {S_i}^T S_i W_i)/\partial(W_i) = 0 \tag{2-14}$$

Please refer to Appendix A for more details on matrix differentiation. The results from equation (2-14) can be expressed as,

$$-\log(d_i)^T S_i - \log(d_i)^T S_i + 2{W_i}^T {S_i}^T S_i = 0 \tag{2-15}$$

And, the solution to equation (2-15) is computed as,

$$W_i = (S_i^T S_i)^{-1} S_i^T \log(d_i) \tag{2-16}$$

The RSSI mapping is created by considering the RSSI values from all BLE beacons in a local network where a smartphone is located. This mapping is updated dynamically to reflect the current environment. Therefore, it could better cauterize the RSSI-distance relationship in a target area.

2.4.2 BLE Distance Estimation

As previously discussed, the large variation of Bluetooth RSSI resulting from noise causes bias error in the RSSI-distance mapping. To improve the robustness of the proposed mapping, we use the SVD methodology as discussed in section 2.3 by defining a mapping relationship as $H_i = [W_1, \ldots, W_n]$, where W_i is the regression weights from equation (2-16). With SVD technique, H_i can be decomposed as,

$$H_i = U \, \Sigma \, V^T \tag{2-17}$$

Where,

$U \in \mathcal{R}\ (n+1) \times (n+1)$ is the orthonormal left singular vectors,

$V \in \mathcal{R}\ (n \times n)$ is the orthonormal right singular vectors, and

$\Sigma = \text{diag}\ (c_1, c_2, \ldots, c_n)$, $c_1, c_2, \ldots, c_n$ are the singular values of the matrix, H_i.

$c_1 \geq c_2 \ldots \geq c_n \geq 0$

The largest singular components in equation (2-17) capture almost only signal information whereas the smallest ones contain almost only noises. The noise reduction can be obtained by adapting a diagonal weighting matrix Γ to equation (2-17).

$$\widehat{H}_i = U\ (\Gamma\Sigma)\ V^T \tag{2-18}$$

Equation (2-18) represents a reconstructed matrix $\widehat{H}_i$ with enhanced RSSI-distance mapping. The weighting matrix Γ can be selected using the least square method by considering the first p singular values as clean mapping and the last $(n-p)$ singular values represents the noise.

$$\Gamma = \begin{bmatrix} \mathrm{I}_p & 0 \\ 0 & 0 \end{bmatrix} \tag{2-19}$$

Where,

I_p is a $p \times p$ identity matrix.

The distance from a smartphone (m) to a BLE beacon (i) can be estimated as,

$$\hat{d}_{m,i} = \exp(S_m \widehat{H}_i) \tag{2-20}$$

Where,

$\hat{d}_{m,i}$ is the estimated distance from smartphone (m) to a BLE beacon (i),

$S_m = [1, s_{m1}, s_{m2}, \dots, s_{mn}]$,

s_{mn} is the RSSI value from smartphone (m) to a BLE beacon (n), and

$\widehat{H}_i$ is the enhanced RSSI-distance mapping.

2.5 POSITION ESTIMATION USING EXTENDED KALMAN FILTER (EKF)

R. E. Kalman (1960) developed a recursive solution to estimate unknown variables based on a series of measurements containing noises and other inaccuracies over time. The Kalman Filter (KF) has been used for guidance, navigation, and control of vehicles and numerous applications in technology. The KF methodology was selected to optimally fuse current position estimates with latest measurement information. We used the KF approach to estimate the location of a Bluetooth scanner based on the received signal strength measurement from its neighboring Bluetooth devices. Based on the knowledge about the uncertainties of the current position estimates and the measurement, the KF combines the information to minimize the estimation error. The geometric relationship between a device and other neighboring devices can be described by equation (2-21) as follows.

$$(X - X_i)(X - X_i)^T = r_i^2 \tag{2-21}$$

Where,

X is the location of a BLE scanner (e.g., a smartphone),

X_i is the location of BLE beacon *i*, and

$\boldsymbol{r_i}$ is the distance between scanner $\boldsymbol{X}$ and sensor $\boldsymbol{X_i}$, $i \in [\mathbf{1}, \mathbf{2}, \dots, \boldsymbol{n}]$.

The extended Kalman filter (EKF) was used for the non-linear system. The location of a smartphone device (X) was selected as the state variables which can be modeled in the following discrete form.

$$X_{k+1} = X_k + w_k \tag{2-22}$$

Where,

X_k (3×1) is the position of BLE scanner at time step t_k,

w_k (3×1) is assumed to be a uncorrelated sequence with known variance $E[w_k w_k^T] = Q_k$.

The observation or measurement of the above discrete process is assumed to occur at discrete points in time according to the following relationship.

$$Z_k = h(X_k) + v_k \tag{2-23}$$

Where,

v_k $(m \times 1)$ is random measurement noise with variance $E[v_k v_k^T] = R_k$,

Z_k $(m \times 1)$ is the range measurement at time step t_k,

m is the number of neighboring Bluetooth devices.

The elements of $h(X_k)$ are the distances between a smartphone device and its neighboring devices, which can be rewritten from equation (2-21) as,

$$h_i(X_k) = \sqrt{(X_k - X_i)^T (X_k - X_i)} \tag{2-24}$$

Where,

$h_i(X_k)$ is the distance between the scanner and the *i*th neighboring Bluetooth device,

i is the index of neighboring device, and

X_i is the location of the neighboring device.

The measurement equation (2-23) needs to be linearized in order to use the discrete KF. Current state estimate is selected as the reference trajectory about which the equations are linearized. Assume ΔX_k is a small difference between the actual position X_k and the current estimate, $\hat{X}_k$. Using Taylor's series expansion with the first order form, the $h(X_k)$ can be linearized as,

$$h(X_k) = h(\hat{X}_k) + H_k \, \Delta X_k \tag{2-25}$$

$$H_k = \left[\frac{\partial h}{\partial X}\right]_{X=\hat{X}_k} \tag{2-26}$$

The rows of the linearized H_k matrix represent a sensor measurement which can be expressed based on the measurement equation (2-24) as follows.

$$h_i^T = -\left(h_i^T - \hat{X}_k\right)^T / \, h_i(\hat{X}_k) \tag{2-27}$$

Based on the theory presented in (Brown & Hwang, 2012), we assume at an initial time, t_k, all estimates were based on knowledge prior to t_k. This prior (or priori) estimate can be denoted as $\hat{X}_k^-$. Therefore, the estimation error can be calculated as,

$$e_k^- = X_k - \hat{X}_k^- \tag{2-28}$$

And the associated error covariance matric is,

$$P_k^- = E\left[e_k^- e_k^{-T}\right] = E[\left(X_k - \hat{X}_k^-\right)\left(X_k - \hat{X}_k^-\right)^T] \tag{2-29}$$

A linear blending of the prior estimate and the noisy measurement can be formulated using the following equation.

$$\hat{X}_k = \hat{X}_k^- + K_k(Z_k - H_k\hat{X}_k^-) \tag{2-30}$$

Where,

$\hat{X}_k$ is the updated estimate

K_k is a blending factor which can be expressed as follows (Brown & Hwang, 2012).

$$K_k = P_k^- H_k^T (H_k P_k^- H_k^T + R_k)^{-1} \tag{2-31}$$

This particular K_k, namely the one that minimizes the mean square estimation error, is called the Kalman gain. The covariance matrix associated with the optimal estimate can, therefore, be computed as,

$$P_k = (I - K_k H_k) P_k^- \tag{2-32}$$

The Kalman filter can be initialized by setting the $\hat{X}_0$ and P_0 to constant values. The first measurement update is evaluated iteratively until a predefined converge criteria are satisfied.

CHAPTER 3: DETECTION OF BLE LOCATION AND NETWORK CONFIGURATION CHANGES

A cumulative summation (CUSUM) methodology and two location change indices were introduced to test if the location of a BLE module is changed or the configuration of the BLE network is altered. The CUSUM technique is to evaluate the location changes of a single BLE module. The Jaccard index and a normalized weighted signal level change (NWSLC) index were used to evaluate the geometry configuration of a local BLE network.

3.1 STATISTICAL PROCESS CONTROL (SPC)

A statistical process control, Cumulative Sum (CUSUM), can be performed to detect and identify any changes of BLE locations. The CUSUM chart is a commonly used quality control method to detect deviations from benchmark values. Hawkins & Olwell (1998) used CUSUM charts and charting as Statistical Process Control (SPC) tools for quality improvement. Luceño (2004) used generalized CUSUM charts to detect level shifts in auto correlated noise. Lin et al. (2007) developed an adaptive CUSUM algorithm to robustly detect anomalies. The cumulative sum of the difference between each measurement and the benchmark value is calculated as the CUSUM value. CUSUM is expressed as follows.

$$C_n = \sum_{i=1}^{n}(X_i - \mu) \tag{3-1}$$

Or in recursive form,

$$C_n = C_{n-1} + (X_i - \mu) \tag{3-2}$$

Where,

X_i is the i[th] data reading from BLE modules

μ is the data mean

C_n is the sum of independent normal $N(0, \sigma^2)$ quantities

The CUSUM equations (3-1 & 3-2) can also be standardized to have zero mean and unit standard deviation as follows.

$$U_i = (X_i - \mu)/\sigma \tag{3-3}$$

$$S_n = \sum_{i=1}^{n} U_i \tag{3-4}$$

Or in recursive form,

$$S_n = S_{n-1} + U_n \tag{3-5}$$

Where,

U_i is the difference of measurement from mean in unit of standard deviation,

S_n is the cumulative difference in unit of standard deviation, and

σ is the standard deviation of a data set.

The cumulative distribution function and the normal inverse cumulative distribution function (illustrated in Figure 3.1) were used before calculating CUSUM. The following equations can be used to calculate the adjusting CUSUM.

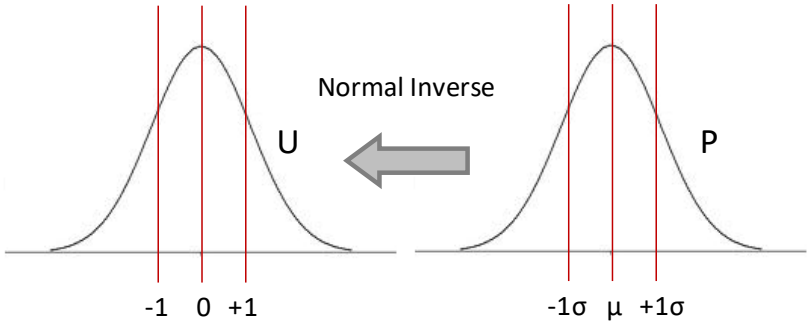

Figure 3.1 Illustration of normal inverse cumulative distribution function.

$$\bar{x}_1 = \frac{\sum_{i=1}^{n_0} \mu_i}{n_0}$$

$$w_1 = \sum_{i=1}^{n_0} (\mu_i - \bar{x}_1)^2$$

$$\bar{x}_{j+1} = \bar{x}_j + \left[\frac{(\mu_{j+n_0} - \bar{x}_j)}{j+n_0}\right]$$

$$w_{j+1} = w_j + (j + n_0 - 1)[\frac{(\mu_{j+n_0} - \bar{x}_j)^2}{j+n_0}]$$

$$\sigma_j^2 = \frac{w_j}{j+n_0-1}$$

$$T_j = \frac{\mu_{j+n_0} - \bar{x}_j}{\sigma_j}$$

$$p_j = tcdf\left(T_j . \sqrt{\frac{j+n_0-1}{j+n_0}}, j + n_0 - 2\right)$$

$$U_j = norminv(p_j, 0, 1)$$

$$adj.cusum_j = \sum_{k=1}^{j} U_k$$

Where,

n = number of measurements,

$n_0 = 3$, initial number of measurements,

w_j is sum of squared difference between individual data and mean,

σ_j^2, is the variance,

$m = n - n_0$,

μ is an array of RSSI average,

$p = tcdf(x, v)$ is the student's t cumulative distribution function (CDF). The result, p, is the probability that a single observation from the t distribution with v degrees of freedom will fall in the interval [–∞, x), and

$U = norminv(p, \mu = 0, \sigma = 1)$ is the normal inverse cumulative distribution function. It computes the inverse of the normal CDF with parameters μ (mean) and σ (standard deviation) the corresponding probabilities in p.

The standardized CUSUM form, S_n (Eq. 3-5), can be used to directly interpret random walks and linear drifts of a process mean. The Decision Interval (DI) of CUSUM is proposed by Hawkins & Olwell to detect a process shift in mean that changes from general horizontal motion to a non-horizontal linear drift. For example, a particular slope k and leg height h can be specified to test a shift. The sequence to monitor an upward shift in mean is defined in equation (3-6 & 3-7) as follows.

$$S_0^+ = 0 \tag{3-6}$$

$$S_n^+ = \max(0,\ S_{n-1}^+ + U_n - \mathrm{k}) \tag{3-7}$$

It signals an upward shift in mean if $S_0^+ > h$. Similarly, the sequence to monitor a downward shift in mean is defined in equation (3-8 & 3-9) as follows.

$$S_0^- = 0 \tag{3-8}$$

$$S_n^- = \min(0,\ S_{n-1}^- + U_n + \mathrm{k}) \tag{3-9}$$

It signals a downward shift in mean if $S_0^- < -h$. The constant k represents a reference value or allowance, and constant h is the decision interval. Hawkins & Olwell described in detail on how to choose an appropriate reference value k for the shift in the mean of a normal distribution. The k value is chosen for the optimal response that the CUSUM process will detect a shift of 2×k standard deviations.

3.2 WIRELESS SIGNAL FINGERPRINT

Trilateration technique has been used by GPS, radar, or other sensors to determine the location of an object. Another positioning technique is called fingerprinting, which is a localization process that represents a radio transmitter by the unique ID and the signal strength at the current location. Wi-Fi fingerprinting has often been used for indoor positioning due to unavailable GPS signals. It requires a robust Received Signal Strength (RSS) database which is used for generating signal strength maps as well as for identifying locations. Each location reference point includes signal strengths measured from all

accessible Access Points (AP). Live RSS data can then be compared to the find the closest match from the database which stores the location of each reference point (Navarro et al, 2011).

Wireless location fingerprinting consists of two phases: the off-line data training and online positioning. Our application does not intend to determine the precise location of a smartphone using wireless fingerprinting. We use the wireless fingerprint positioning process to determine the *change* in location of a BLE module, which allows for a much more efficient use of BLE data (Liao et al., 2016). Importantly, our approach does not require the additional layer of complexity incurred by the need to compose and maintain external RSS databases as well as querying them for each location determination. In particular, the BLE module can record the wireless fingerprint when the network was installed. The scanned BLE signals were stored in the cloud and will be used as a reference signature. When a BLE module detects any suspicious movement using the CUSUM methodology, the app on a user's smartphone will inform the server to compare the current BLE signal fingerprint with the stored reference to determine and validate if the location of a BLE module is changed.

Each record from the BLE scan result list includes MAC address and Received Signal Strength Indication (RSSI). The MAC address is a unique identifier associated with each BLE module. The RSSI is the received signal strength from the corresponding BLE module. RSSI is expressed in dBm which is defined as the power ratio in decibels (dB) of the measured power referenced to one milliwatt (mW) as displayed in Equation (3-10).

$$dBm = 10log_{10}\frac{Power}{1mW} \tag{3-10}$$

The RSSI signal strength in dBm can be converted into a discrete *N*-level signal indication (where $N = 5$ is a commonly used value), often displayed using bars on smartphone screens. The Android API provides a function to compute signal strength level based on the RSSI,

$$SigLevel = WifiManager.calculateSignalLevel\ (RSSI,\ N) \tag{3-11}$$

Where,

RSSI is the measured signal strength in dBm,

N is the total number of signal levels, and

$SigLevel \in \{0,1,\dots,\mathrm{N}-1\}$.

Our proposed approaches use MAC ID and Received Signal Strength Indication (RSSI) elements of the BLE fingerprint. That is, a BLE fingerprint F_x of at given location x is represented as $F_x = \{(MAC_i, RSSI_i)\}$, where each tuple $(MAC_i, RSSI_i)$ indicates a specific (i^{th}) BLE network (ID and signal strength) visible at location x.

3.2.1 Jaccard Index

The Jaccard index, or similarity coefficient, was previously developed by Paul Jaccard to compare regional floras. The similarity index is also widely used in data-mining (Rajaraman and Ullman, 2011) for comparing the similarity and diversity of a finite number of sample sets. Specifically, the similarity of two sets S_1 and S_2 is defined as:

$$J(S_1, S_2) = \frac{|S_1 \cap S_2|}{|S_1 \cup S_2|} \in [0,1] \tag{3-12}$$

In our case, S_1 and S_2 are the reference MAC ID list and the current MAC ID list, respectively. More specifically, given two Wi-Fi fingerprints F_1 and F_2 from two different locations, S_1 and S_2 are defined to include MAC IDs of only those networks that have a signal level (ranging from 0 to 4) equal or greater than 1 for Jaccard index calculation. Formally,

$$S_i = \{\, MAC\ ID \mid (MAC\ ID, RSSI) \in F_i, SigLevel\,(RSSI, 5) \geq 1 \,\}, \qquad \text{for } i = 1, 2.$$

That is, this approach uses the changes in the fingerprint of the strong-signal networks (with a signal strength of 1 or higher) for location change determination. By definition, the value of $J(S_1, S_2)$ is always between 0 and 1. We define that the location of a smartphone is changed when the Jaccard index drops below some threshold $J_{threshold}$, i.e., $J(S_1, S_2) < J_{threshold}$, which essentially indicates that the overlap between two sets of Wi-Fi networks from scans F_1 and F_2 is minimal.

3.2.2 Normalized Weighted Signal Level Change

We also introduce an alternative (somewhat more sophisticated) measure called normalized weighted signal level change is introduced and formulated by the authors for location change detection. NWSLC describes the changes of a network signature by weighting the signal level differences between the reference (from F_1 scan) and current (from F_2 scan) signal level with its reference signal strength and then taking the normalized average. It is defined as follows.

$$A = \frac{1}{Nn} \sum_{i=1}^{n} SigLevel_{ref_i} \times \left| SigLevel_{cur_i} - SigLevel_{ref_i} \right| \tag{3-13}$$

Where,

A is the NWSLC index,

n is the number of intersection samples (i.e., $n = |\, F_1 \cap F_2 \,|$),

N is the total number of signal levels (i.e., $N = 5$ in our case),

$SigLevel_{ref_i}$ is the signal level of reference AP i (from scan F_1), and

$SigLevel_{cur_i}$ is the signal level of current AP i (from scan F_2).

We define that the location of a smartphone is changed when the NWSLC index is larger than a certain threshold $A_{threshold}$, i.e., $A \geq A_{threshold}$, which takes into account not only the change in visible Wi-Fi networks but also the relative change in their signal strength.

CHAPTER 4: SOLAR-POWERED BLE SYSTEM

This chapter describes the integration of a solar-power Bluetooth Low Energy (BLE) system using commercial off-the-shelf (COTS) solar panel and charging system. A simple mounting system was also designed and developed for the solar panel.

4.1 SOLAR CHARGER SYSTEM

In the literature, Jeon et al. (2016) identified the challenges of finite battery capacity for BLE beacons used in the Internet of Things (IoT) applications. They conducted a preliminary design of sustainable BLE beacons powered by solar panels. Their results indicated that a typical BLE beacon can be powered by a solar panel with a surface area of 300 cm^2 and a lithium-ion rechargeable coin cell battery. In addition, Spachos and Mackey (2018) evaluated the energy efficiency and accuracy of the solar-powered BLE beacons by comparing the solar vs. battery powered BLE beacons. Their results indicated that the solar-powered BLE beacon is a promising solution with minimum energy requirement and high accuracy.

A solar charging system was integrated and packaged in a National Electrical Manufacturers Association (NEMA) polycarbonate enclosure as illustrated in Figure 4.1. The solar charging system is comprised of a 3.7V 4400 mAh Lithium-Ion Polymer (LiPo) battery, a Li-Ion / Li-Polymer battery charge circuit board based on Microchip MCP73833, and a 6V solar panel. The battery charging system is configured to have a maximum charging rate of 500 mA. The design was designed to draw the most current possible from a solar cell, up to the max charge rate. It's also capable of autonomous power source selection between an input (from DC, USB, or solar) or a battery.

There are three status LEDs on the LiPo charger. The red PWR LED indicates that there is good power connected to the charger. The orange CHRG LED indicates current charging status. When this LED is lit, the charger is working to charge up a battery. It also acts as a low battery indicator (fixed at 3.1V) when no power is connected. That is, when the battery voltage drops below 3.1V, the orange LED will come on. The green DONE LED indicates the battery is charged when it's lit up.

The smart load sharing function automatically uses the input power when available to keep the battery from constantly charging or discharging. The LiPo charger is both charging a battery and providing power to the BLE beacon at the same time.

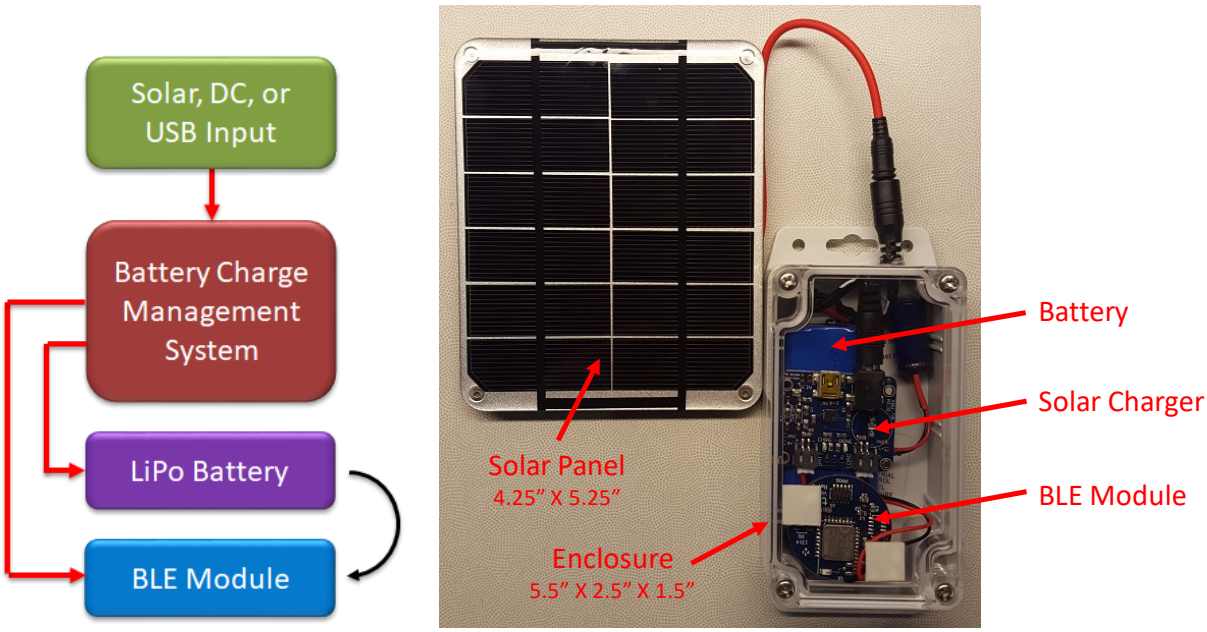

Figure 4.1 Solar charger system for a BLE beacon.

4.2 DESIGN OF SOLAR PANEL MOUNTING FIXTURE

A solar panel mounting system was designed and created using aluminum angle bars. The fixture design allows installers to easily adjust the tilt angle of the solar panel for maximum energy yield. As displayed in Figure 4.2, the solar panel with the customized mounting fixture was attached to a street lamp post using a stainless steel clamp. Detailed design drawings of the mounting fixtures are included in Appendix B. Figure 4.3 displays a complete solar-powered BLE system mounted on a street light post using worm gear clamps. Figure 4.4 displays the installation of solar-powered BLE beacons on street light posts in downtown St. Paul, MN.

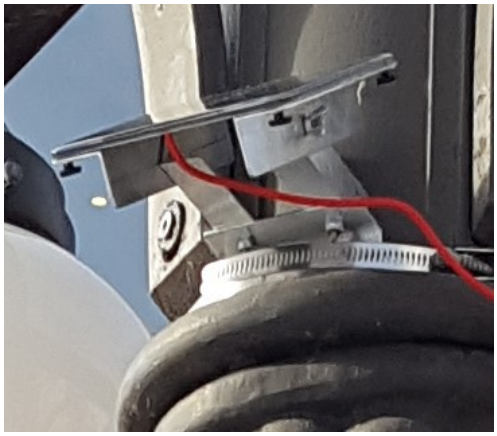

Figure 4.2 Solar panel mounting assembly.

Figure 4.3 Solar-powered BLE on a street light post.

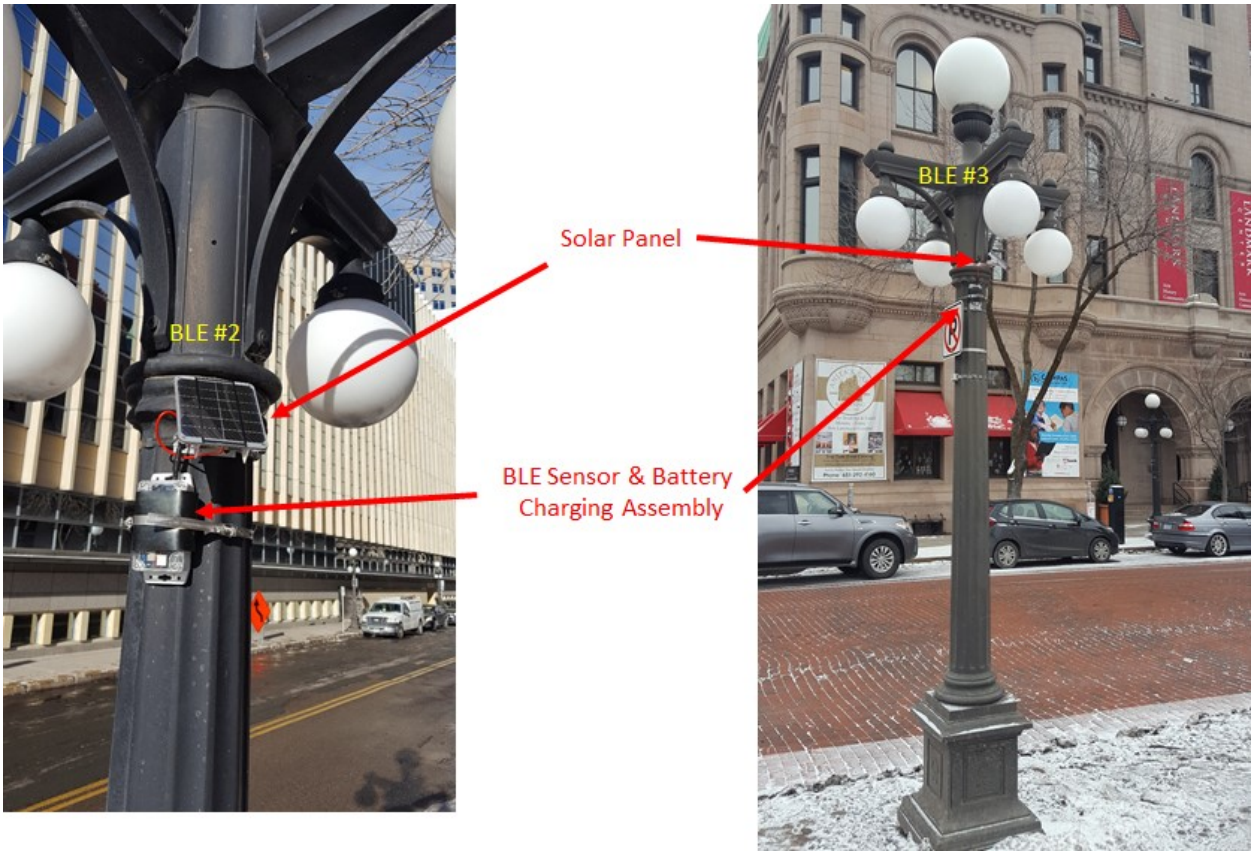

Figure 4.4 Installation of solar-powered BLE beacons in St. Paul, MN.

Six solar-powered BLE beacons were installed at an un-signalized intersection (W 5th St & Washington St) in Downtown St. Paul, MN on 12/7/2017. All BLE beacons have survived through this past winter season with 22 days of the lowest temperature below 0F and the lowest temperature is -15F on 12/31/2017. Experiment results of using BLE beacons for local positioning are discussed in the following Chapter.

CHAPTER 5: EXPERIMENT RESULTS AND ANALYSIS

We reprogrammed the firmware of commercial off-the-shelf Bluetooth Low Energy (BLE) beacons for our experiments. The characteristics of the Received Signal Strength Indication (RSSI) were examined. Four BLE beacons were installed at an intersection to evaluate the positioning and mapping methodology as discussed in Chapter 2 using RSSI. Statistical methodologies discussed in Chapter were also tested to validate the capability of a self-aware BLE network.

5.1 PROGRAM BLUETOOTH LOW ENERGY (BLE) BEACONS

The low-cost Bluetooth Low Energy (BLE) devices have enabled many applications using BLE tags and smartphone devices to locate or identify a personal item, or alert owners when personal belongings are left behind. Some applications use crowdsourcing to help retrieve lost items when the items are out of the owners' Bluetooth communication range. However, these BLE tags, primarily designed to be detected or discovered, do not communicate with each other.

We developed a standalone Bluetooth smart system (called BLE-smart) that integrates a commercial off-the-shelf BLE module operating in dual modes (master/slave or scanning/advertising) with necessary interface elements to sense other BLE-smart devices within its range of communication. The BLE-smart units will remember and periodically check the other BLE-smart devices in their communication range to ensure the integrity of the local map and to provide correct positioning information in an environment.

A Texas Instruments (TI) CC2540 development kit (including CC debugger) was acquired and used to program the BLE modules (as illustrated in Figure 5.1).

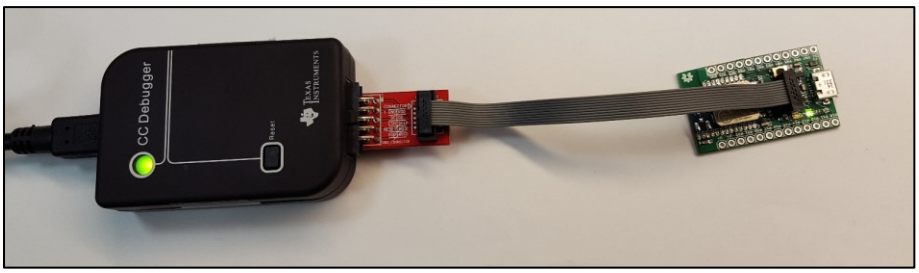

Figure 5.1 TI CC debugger and a BLE module.

The generic attribute (GATT) layer of the Bluetooth 4.x protocol stack is used by the application for data communication between two BLE devices when one of them acts as a GATT server and the other as a GATT client. A GATT server consists of one or more GATT services, which are collections of data to accomplish a particular function or feature. "Characteristics" are values that are used by a service, along with properties and configuration information. GATT defines the sub-procedures for discovering, reading, and writing attributes over a BLE connection. The characteristic values, along with their properties and their configuration data (also known as "descriptors") on the GATT server are stored in the attribute table. Figure 5.2 illustrates our implementation (in blue font) of the GATT server and service on each BLE device. Each BLE device is programmed to be in central mode (master) for 10

seconds after which it switches to peripheral mode (slave) and remains in that role for 50 seconds. When in the central mode, the application searches for surrounding BLE devices that are programmed for our application and gets their corresponding MAC addresses and RSSI values and stores them locally. When in the peripheral mode, the application hosts a GATT server with the GATT service and is ready to be connected to a central device. The GATT service hosts the device MAC addresses and RSSI values previously read in the central mode. A central BLE device (for example, a smartphone) can now connect to the device in peripheral mode and read the values of MAC addresses and RSSI values of its neighboring BLE devices from the GATT server.

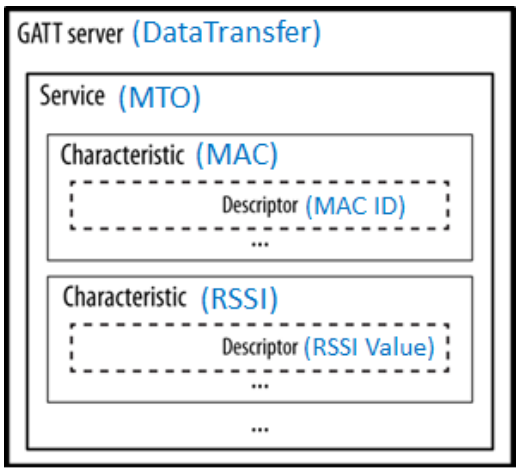

Figure 5.2 GATT services running on each BLE module.

A Smartphone app was also developed for data collection and testing as displayed in Figure 5.3. It illustrates one of the BLE devices when operating in master/scanning mode detects 3 other BLE devices in its vicinity.

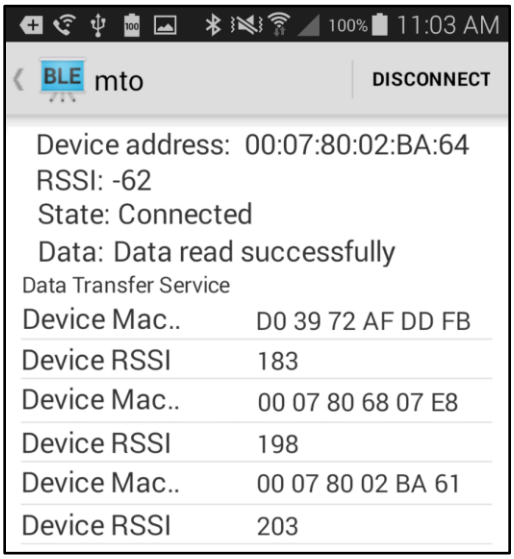

Figure 5.3 Image of a smartphone app for testing.

We tested the reprogrammed BLE beacons and explored the relationship between actual distance and the RSSI values in the atrium of the Ralph Rapson Hall on University of Minnesota east bank campus. A layout of the reference points and placement of four BLE devices (located at A, D, M & P) are illustrated in Figure 5.4. The relationship between the RSSI reading and actual distance to each Bluetooth device is plotted in Figure 5.5. The results suggest a logarithmical relationship between the measured RSSI and actual distance. However, the distance estimation based on measured RSSI has a relatively low coefficient of determination (R2 = 0.14). The distance estimation based on RSSI measurement is not reliable.

A concept of BLE fingerprinting is introduced to monitor the changes of RSSI values received from other Bluetooth devices. The RSSI signal fingerprint of Bluetooth devices at each test location is displayed in Figure 5.6. When a Bluetooth device is operating in scanning (master) mode and monitoring its neighboring devices, the measured RSSI signals from all the other Bluetooth devices within its range of communication are stored in local memory. If one of the neighboring Bluetooth devices is moved, vandalized or malfunction, the fingerprint pattern at that particular location will be different from the historical pattern. Therefore, an alert can be triggered to inform the system administrator.

For example, the average RSSI measurements from the other four Bluetooth devices at location F is displayed in a column chart as shown in Figure 5.7(a). The red ticks plotted on each column represent the RSSI value of one standard deviation above and below the average measurement. Similarly, the fingerprint of the RSSI values and corresponding variations at location G (as shown in Figure 5.4) is shown in Figure 5.7(b). Each of these fingerprints is used to determine if any of the neighboring Bluetooth devices (MTO-07 ~ MTO-10) has been removed or stopped functioning. When a user approaches the BLE device with the Smartphone app running in the background, the BLE fingerprint information will automatically be transferred to a database server through the wireless services on the smartphone.

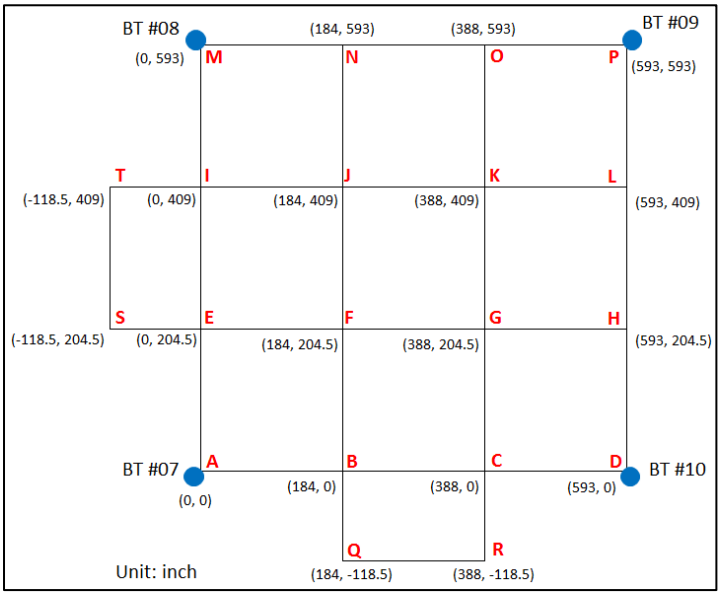

Figure 5.4 RSSI data collection and validation.

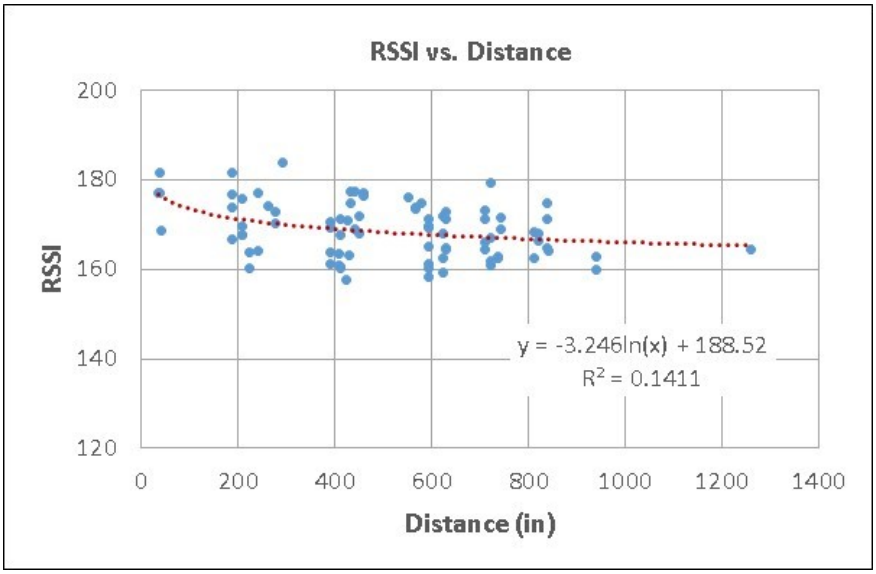

Figure 5.5 RSSI measurement vs. distance (indoor).

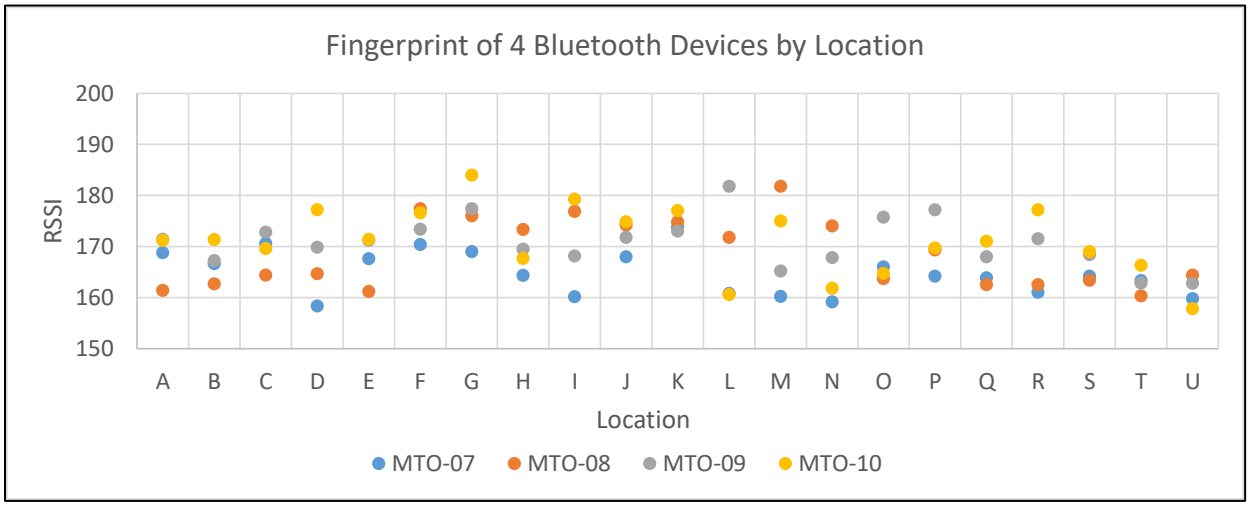

Figure 5.6 Average RSSI values of 4 Bluetooth devices by location.

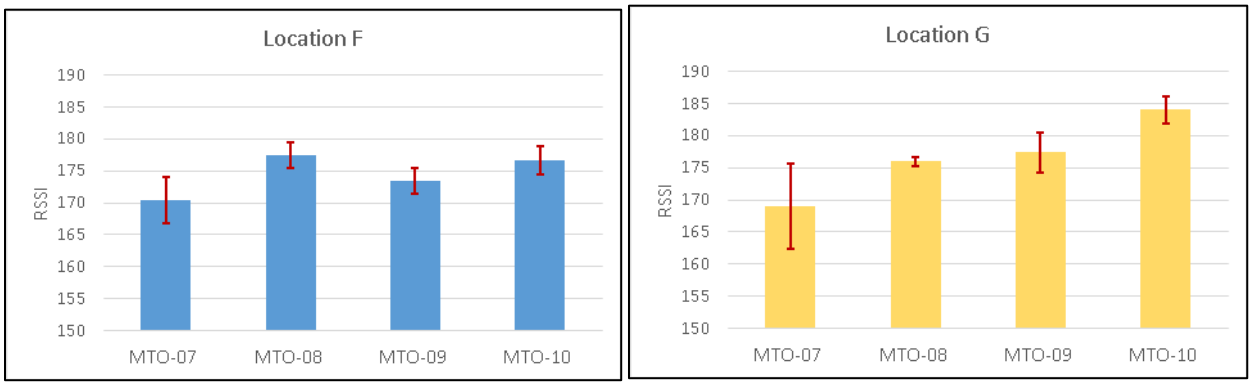

Figure 5.7 RSSI measurement and variation of 4 BLE beacons at location F and G.

A similar analysis for 12 BLE beacons placed in an outdoor environment was also conducted to examine the RSSI-distance relationship as displayed in Figure 5.8. RSSI measurements from BLE beacons may vary by locations due to the environmental dynamics and nature of Bluetooth wireless medium.

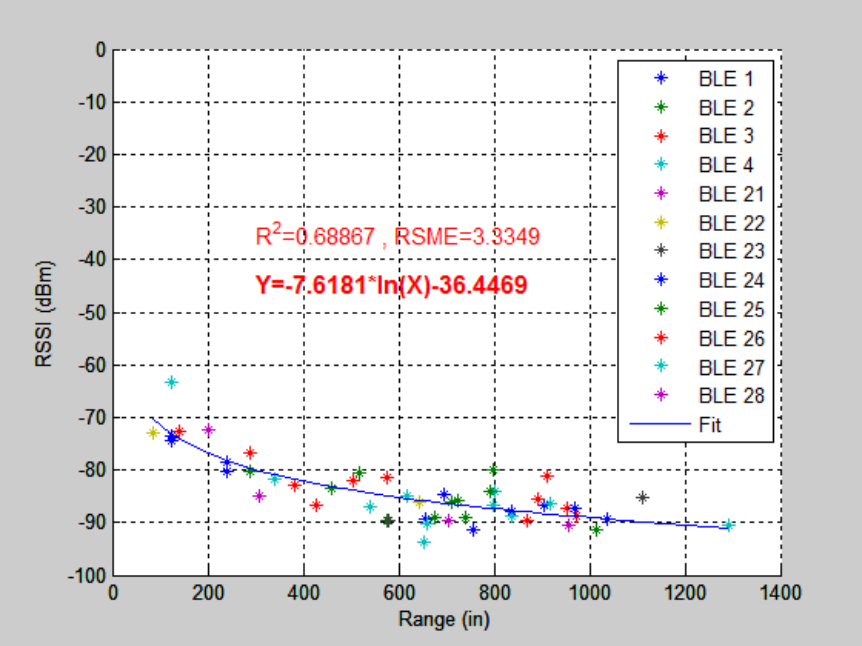

Figure 5.8 RSSI vs distance relationship (outdoor).

5.2 GEOSPATIAL DATABASE

A geospatial database that contains the location and corresponding message of each BLE device was developed to provide information to a smartphone app. As illustrated in Figure 5.9, the BLE network will be built upon the street network. Each BLE parent node includes a MAC ID, latitude, longitude, and information of its neighboring nodes which may be located on the other side of the street of the next block. The relation between a parent and a child node describes relative orientation, direction, crosswalk and street information. The goal is to provide reliable situation awareness and corresponding navigation information to assist wayfinding for the visually impaired. The spatial relationship is to ensure that correct audible information (such as signal timing and intersection geometry) is provided to users at the correct location.

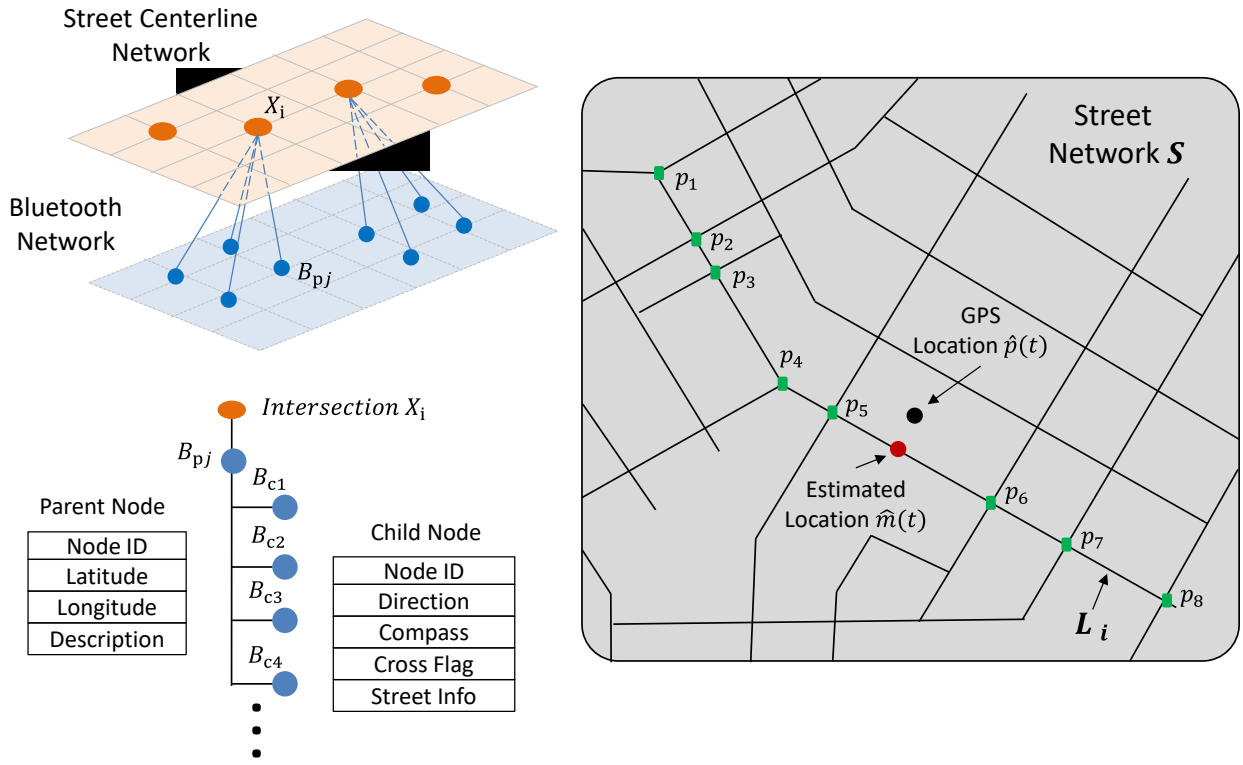

Figure 5.9 Illustration of a geospatial database.

5.3 RSSI MAPPING AND POSITIONING

The BLE beacons were installed at two un-signalized intersections in St. Paul, MN for testing the positioning accuracy of the BLE network. Lithium coin cell batteries (e.g., CR2032) were used in the first intersection using four beacons. Six solar-powered BLE beacons were installed at the second un-signalized intersection. Experiment results are discussed in the following sections.

5.3.1 Using 4 Beacons Powered by Coin Cell Battery

Four Bluetooth low energy beacons were installed at an intersection (Judson Ave. and Underwood St.) in St. Paul as illustrated in Figure 5.10. Nine reference points (location A to I) were selected as position references. Figure 5.11 displays a sample of noisy RSSI signals received from 4 other BLE beacons at location G (as shown in Figure 5.10) using a smartphone.

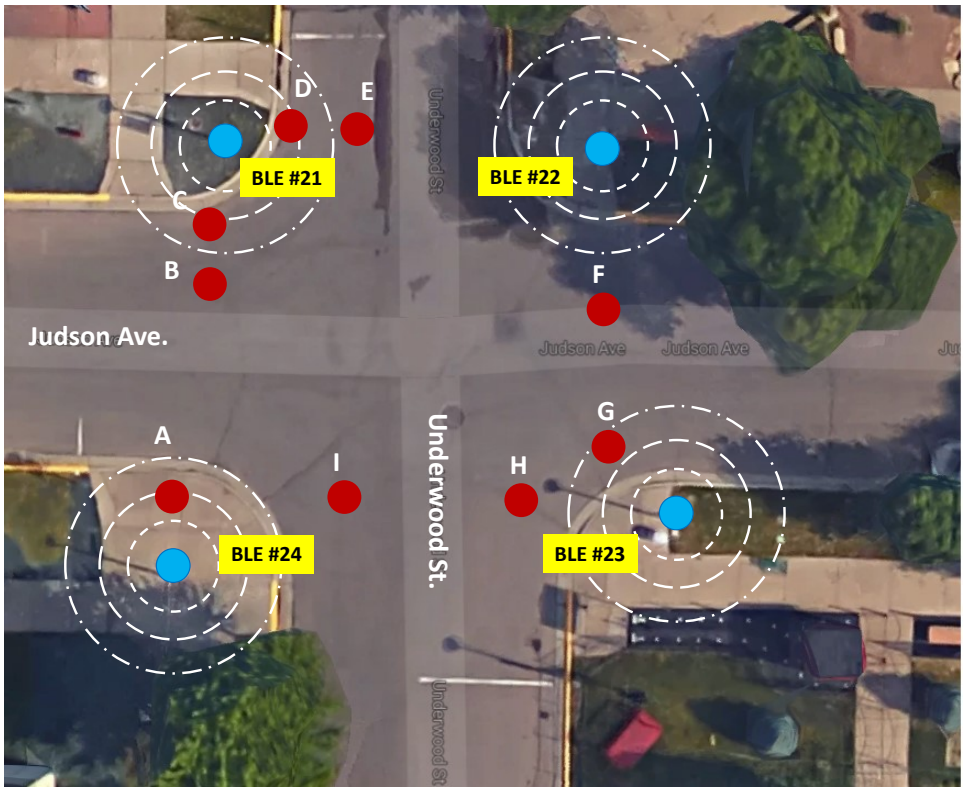

Figure 5.10 A simple Bluetooth network (background image from Google maps).

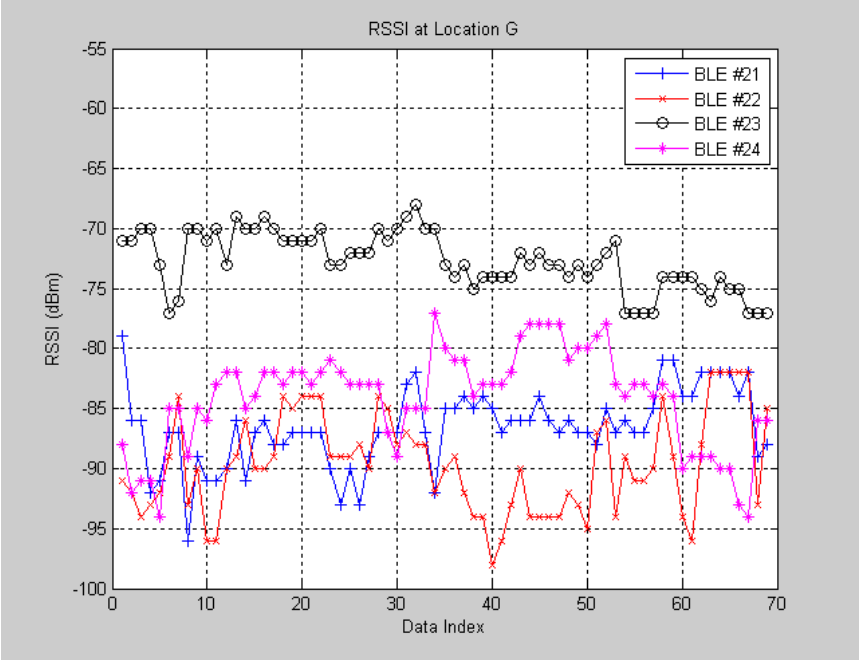

Figure 5.11 Sample RSSI measurements from 4 other BLE beacons at location G.

We first tried a Logarithmic Curve Fitting (LCF) based RSSI-range model for positioning solution. The results were not good. We then implemented the Multivariable Regression (MR) model (discussed in

chapter 3) to estimate the actual distance between BLE beacons. One minute of RSSI data was collected at all 9 locations (A~I) using a smartphone app at the test site as illustrated in Figure 5.10. Each collected dataset include RSSI received from all other neighboring BLE beacons. The estimated distance between the smartphone and each BLE beacon is then used by the Extended Kalman Filter (EKF) (discussed in chapter 2.5) to determine the location of a smartphone. Table 5.1 compares the average absolute position error of the 9 locations for both models. The LCF and EKF combined model has an absolute position error of 7.3 m (X-axis) and 9.5 m (Y-axis), respectively. The MR and EKF combined model improves the position error by about 44% with an absolute position error of 4.1 m (X-axis) and 5.4 m (Y-axis), respectively.

Table 5.1 Comparison of absolute position error using different methodologies

Absolute Position Error (m)		
Direction	X Axis	Y Axis
LCF + EKF	7.3	9.5
MR + EKF	4.1	5.4
% Change	-44.1%	-43.6%

5.3.2 Using 6 Solar-Powered Beacons

Six BLE beacons were installed at an un-signalized intersection (Washington St and W 5th St) in downtown St. Paul as illustrated in Figure 5.12. Five reference points (location A to F) were selected as position references. One minute of RSSI data was collected at all 5 locations (A to F) using a smartphone app at each location illustrated in Figure 5.12. Each collected dataset include RSSI received from all other neighboring BLE beacons. The estimated distance between the smartphone and each BLE beacon is then used by the trilateration methodology to determine the location of the smartphone. The position solution using 6 BLE beacons at the second location is better than the results from the first intersection using only 4 beacons. The absolute position error is respectively 2.5 m (SD: 2.3 m) in X-axis and 3.8 m (SD: 1.7 m) in Y-axis. Using 6 beacons improves the position error by about 30 to 39% as listed in Table 5.2.

Table 5.2 Comparison of absolute position error using more beacons

Absolute Position Error (m)		
Direction	X Axis	Y Axis
Using 4 BLE Beacons	4.1	5.4
Using 6 BLE Beacons	2.5	3.8
% Change	-39.0%	-29.6%

Figure 5.13 displays a sample of noisy RSSI signals received from 6 other BLE beacons at location D (as shown in Figure 5.12) using a smartphone.

Figure 5.12 A Network of 6 BLE Beacons installed in downtown St. Paul, MN.

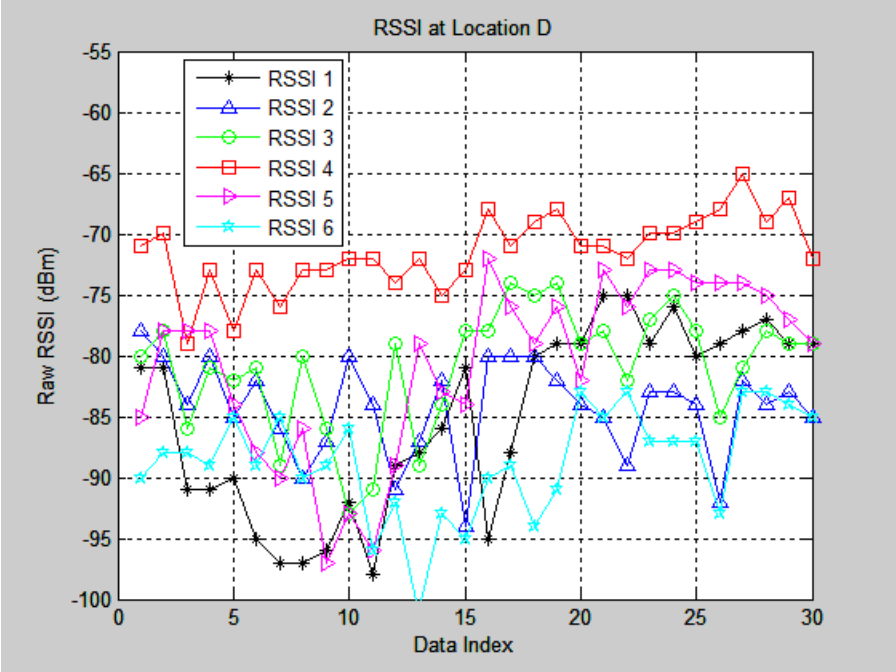

Figure 5.13 Sample RSSI measurements from 6 other BLE beacons at location D.

5.4 CUSUM ANALYSIS FOR DETECTING BLE LOCATION CHANGES

In order to detect the change of location of a BLE beacon or changes of a BLE network geometry, the methodologies described in section 3.1 were used for validation. Experiments were conducted by moving one of the BLE beacons at a 3-meter increment in both lateral and longitudinal directions. Figure 5.14 displays the CUSUM and Decision Interval (DI) plots of a BLE beacon (for example, BLE #22, as shown in Figure 5.10) was moved away from its neighboring node (BLE #21) for about 6 meters after 50 seconds (250 samples). The CUSUM algorithm is able to detect changes of RSSI shortly after the displacement of BLE #22 beacon.

Statistically, test results of moving the BLE tags are listed in Table 5.3. The CUSUM detection algorithm is able to detect the location changes of a peer BLE tag at 3 meters range 86% of the times. The CUSUM detection rate increases to 100% when a BLE tag is moved over 6 meters away from its peer.

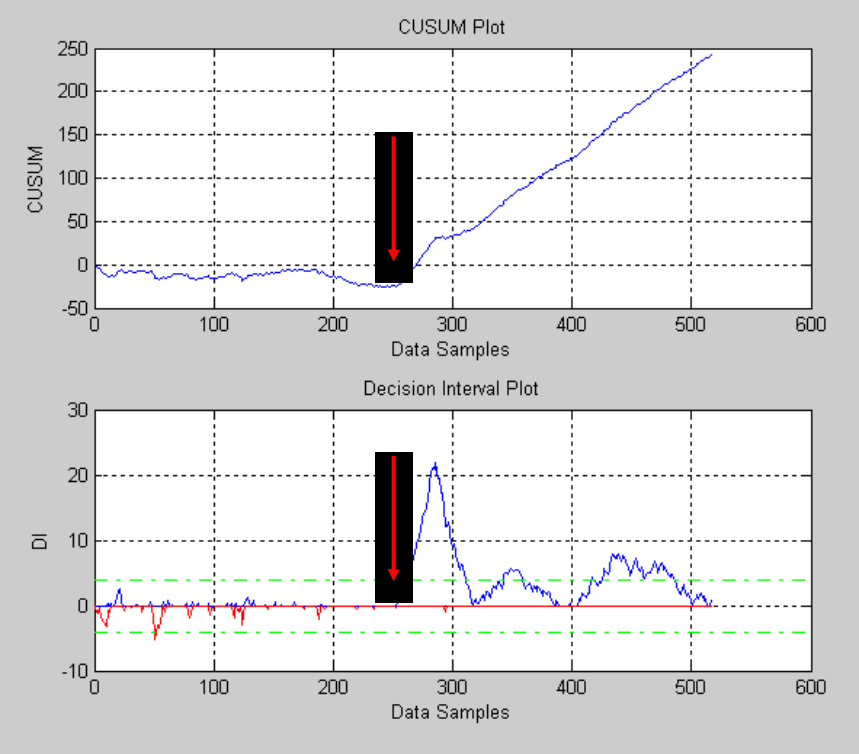

Figure 5.14 CUSUM and DI plots of a BLE moved away from its neighboring node.

Table 5.3 CUSUM test results of moving BLE tags

CUSUM Detection	Move away from a peer		Move toward a peer	
Starting Location (m)	+3 meters	+6 meters	-3 meters	-6 meters
3	Yes	Yes	NA	NA
6	No	Yes	Yes	Yes
9	Yes	Yes	No	Yes
12	Yes	Yes	Yes	Yes

15	Yes	Yes	Yes	Yes
18	Yes	Yes	Yes	Yes
21	Yes	Yes	Yes	Yes
24	Yes	Yes	Yes	Yes
27	Yes	Yes	Yes	Yes
30	Yes	Yes	No	Yes
33	Yes	Yes	Yes	Yes

5.5 RSSI FINGERPRINT FOR BLE NETWORK CONFIGURATION CHANGES

We validated both RSSI signal fingerprint techniques as discussed in chapter 3.2. Figure 5.15 shows the Jaccard index signature of the Judson Ave. and Underwood St. intersection displayed in Figure 5.10 when all 4 BLE beacons are mounted at their original locations. When BLE #21 is removed from the network, the RSSI fingerprint changes and the average Jaccard index drops from 0.98 to 0.82 as shown in Figure 5.16. Similarly, the average Jaccard index drops from 0.98 to 0.53 (as plotted in Figure 5.17) when BLE #23 is removed from the network.

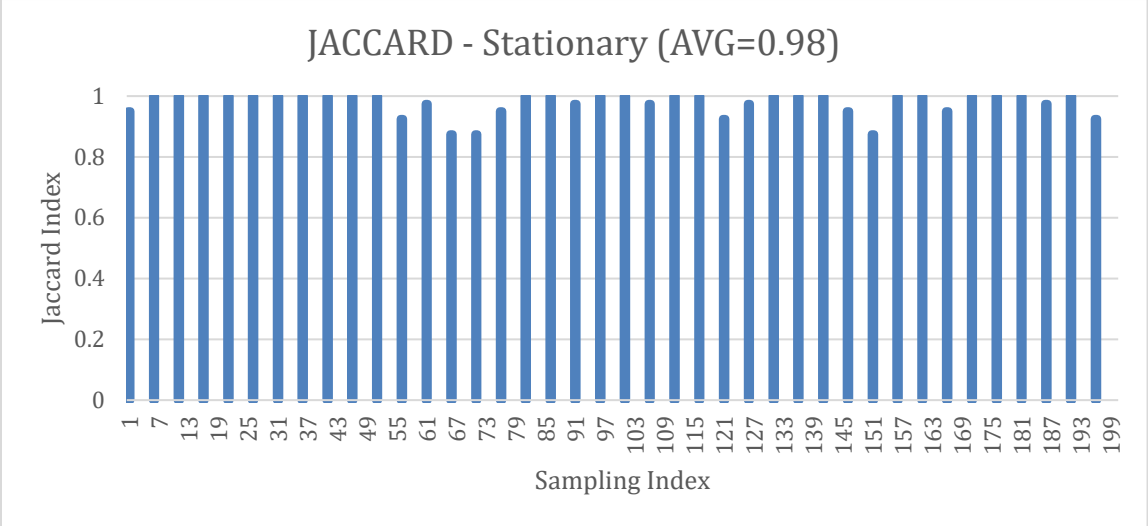

Figure 5.15 Jaccard Index in normal condition.

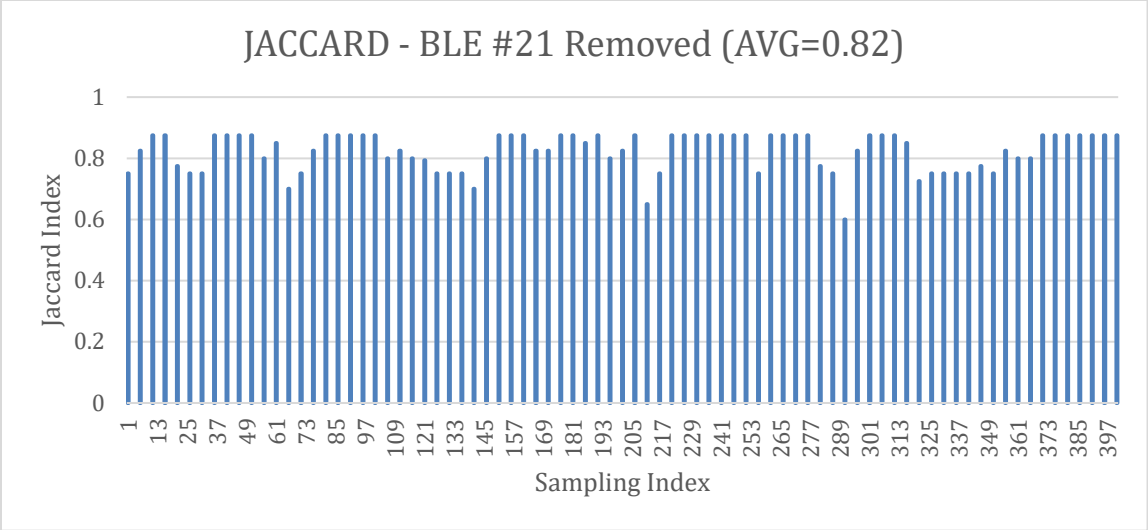

Figure 5.16 Jaccard Index when BLE#21 was removed.

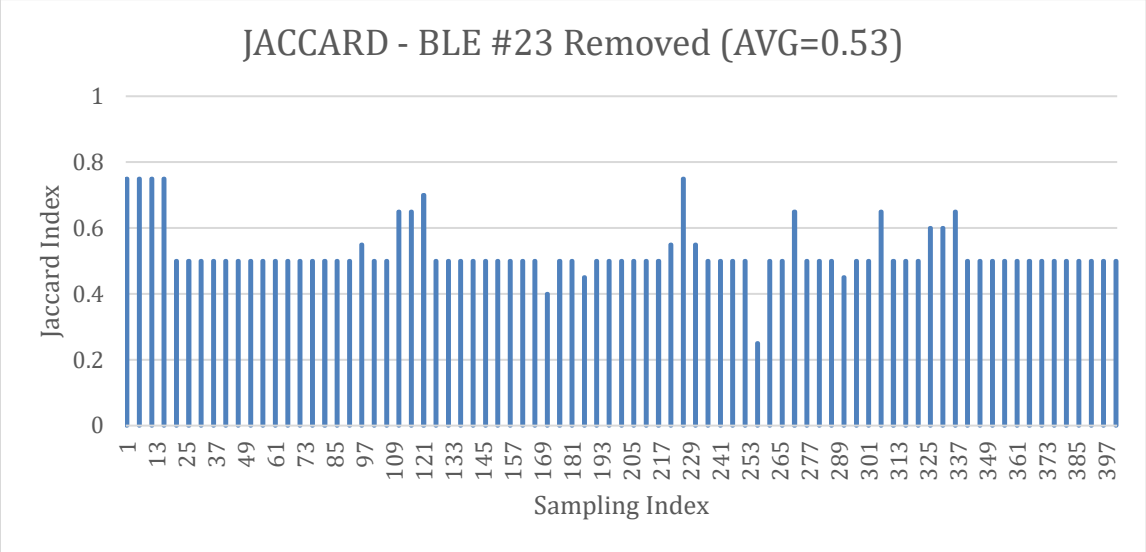

Figure 5.17 Jaccard Index when BLE#23 was removed.

The NWSLC index (from equation 3-13) was also examined at the same intersection. Figure 5.18 illustrates the NWSLC index when all BLE beacons are at their original locations based on 196 sets of RSSI measurements. The average NWSLC is 0.15 with a standard deviation (SD) of 0.09. When the BLE #23 is moved 5 meters away, the NWSLC signature changes with an average index increased to 0.62 and its SD is 0.24, as shown in Figure 5.19. Our fingerprint method used a two-tailed t-test (at the 95% confidence interval) to confirm a significant change of the NWSLC index pattern. Similarly, the NWSLC index in Figure 5.20 increases to 0.91 on average with an SD of 0.28 when the BLE #23 beacon is removed from the self-monitoring BLE network.

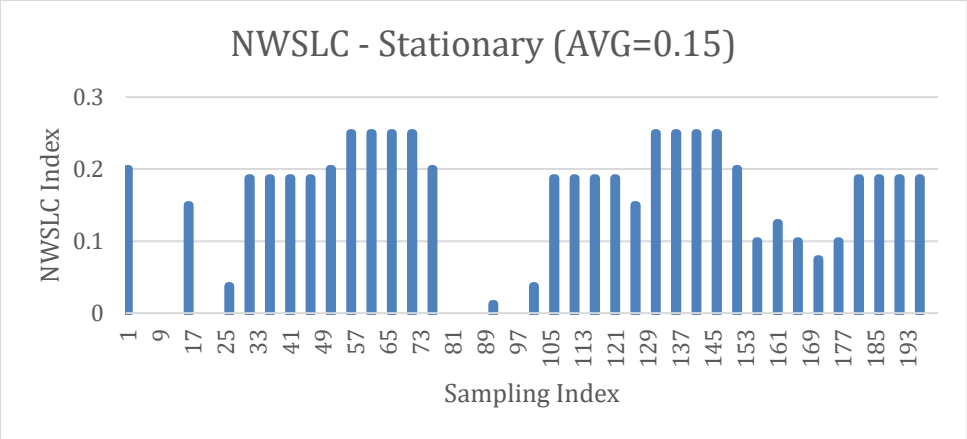

Figure 5.18 NWSLC index in normal condition.

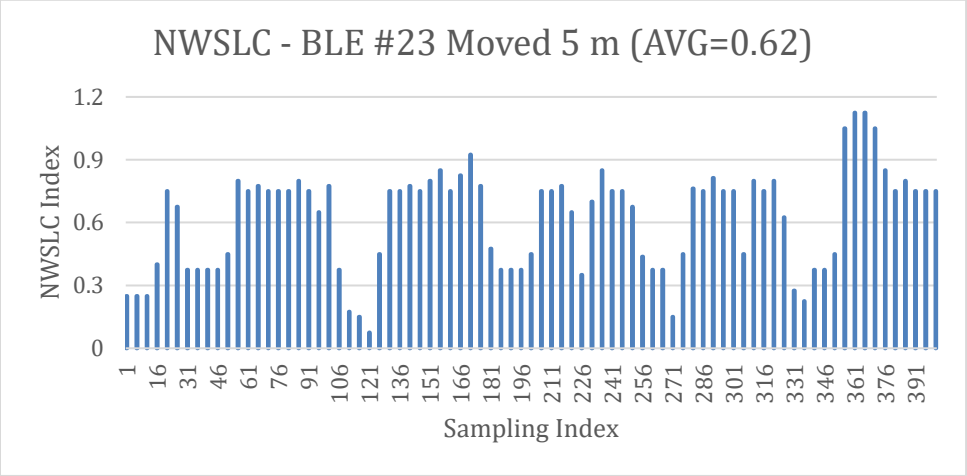

Figure 5.19 NWSLC index when BLE #23 was moved by 5 m.

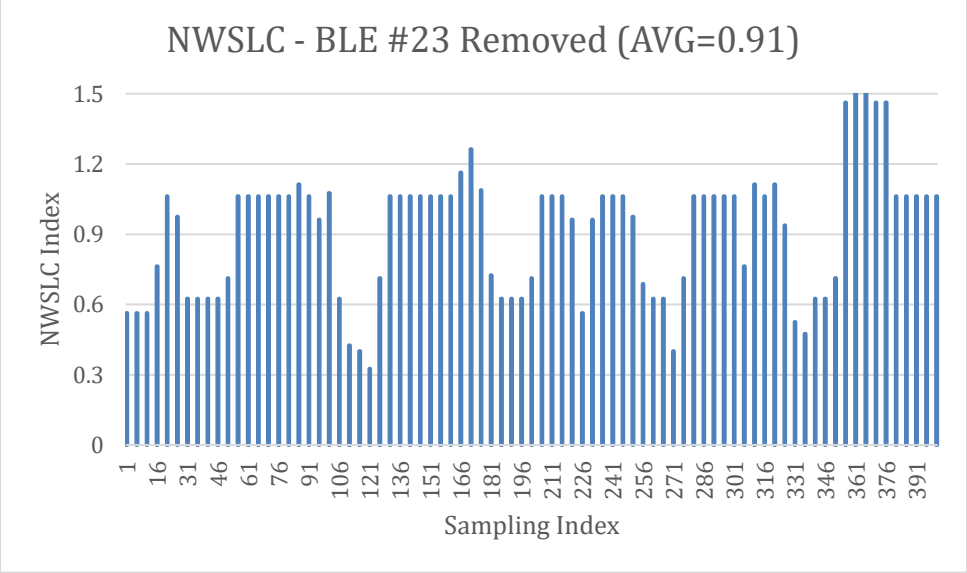

Figure 5.20 NWSLC index when BLE #23 was totally moved.

CHAPTER 6: SUMMARY

After receiving orientation and mobility (O&M) training from O&M specialists, people with vision impairment can often travel long, complex, and novel distances independently. Some blind pedestrians use a white cane or guide dog as their primary tool for obstacle detection while traveling. Environmental cues, though not always reliable, are often used to support the wayfinding and decision making of the visually impaired at various levels of navigation and situation awareness.

Most of the people who are blind or visually impaired travel without any major barriers. However, some pedestrians who are blind could encounter physical and information barriers that limit their transportation accessibility and mobility. To improve their mobility, accessibility, and level of confidence in using the transportation system, it is important to remove not only the physical barriers but also the information barriers that could potentially impede their mobility and undermine safety.

In this report, we described a position sensing and a self-monitoring infrastructure to ensure the information provided to the visually impaired is up to date and at the right location. We developed a method that uses the ability of a smartphone with Bluetooth to sense the proximity of Bluetooth modules and their ability to sense each other. For positioning and mapping, we evaluated two methodologies, Logarithmic Curve Fitting (LCF) and Multivariable Regression (MR), to find a robust positioning solution to identify a user's relative location near an intersection. Our results indicated that the MR method using Singular Value Decomposition (SVD) algorithm outperforms the LCF method in modeling the relationship between Received Signal Strength Indication (RSSI) and the actual ranging distance in an outdoor environment. The MR-SVD approach successfully reduces the environmental uncertainty and dynamic nature of the RSSI measurements. The range output from the MR-SVD model is integrated with an Extended Kalman Filter (EKF) model to determine a user's location.

We initially conducted experiments at an un-signalized intersection on the Minnesota State Fairgrounds in St. Paul using 4 battery-powered BLE beacons. Due to the significant noise associated with the RSSI measurements, the LCF model has large position errors (7.3 and 9.5 m in X and Y axis, respectively). The MR-SVD and EKF combined model improves the position error by about 44% (to 4.1 and 5.4 m in X and Y axis, respectively). Additional experiments were later conducted at another test site in downtown St. Paul, Minnesota, using 6 solar-powered BLE beacons. The position accuracy was further improved to 2.5 and 3.8 m in X and Y axis, respectively

Because of the low power characteristics of the BLE beacons, the received signal strength is subject to influences from many external parameters. Although the positioning performance of the MR-SVD and EKF combined method is not sufficient for detecting pedestrian veering at crosswalks, it provides reasonable positioning to identify a person's location at a corner of an intersection in a GPS unfriendly environment.

To create the self-monitoring infrastructure, a Cumulative Sum (CUSUM) technique is implemented to monitor whether the location of one or multiple BLE beacons in a network is changed based on Bluetooth RSSI measurements. Our results indicate that the CUSUM detection algorithm is able to

detect the range changes of a peer BLE beacon of 3 meters 86% of the time. The CUSUM detection rate increases to 100% when a BLE tag is moved over 6 meters away from its original location.

In addition, we evaluated two wireless signal fingerprinting indices, the Jaccard and Normalized Weighted Signal Level Change (NWSLC) indices, to detect geometry changes of a BLE network. Both indices were able to successfully detect the change of a BLE beacon when it was moved 3 to 6 meters away, removed or disappeared (e.g., due to vandalism or lost power) from a network. However, the NWSLC index performs better than the Jaccard index. It normalizes the changes of a signal based on its initial signal states. As a network geometry configuration changes, the NWSLC index increases proportionally to the amount of change with respect to its initial signal strength.

The combined MR-SVD and EKF methods are incorporated into our system for positioning. The CUSUM and NWSLC techniques are both incorporated into our system for self-monitoring infrastructure. The CUSUM is used to detect changes between 2 BLE beacons. And, the NWSLC index is used to monitor the changes of BLE network geometry.

The self-monitoring feature ensures the information provided to users is correct. It reports BLE network status automatically to the system administrator and reduces the maintenance required for public agencies. The crowdsourcing technique sends BLE information from a local network back to the cloud server using a user's smartphone network.

6.1 SYSTEM BENEFITS

Our system can be deployed on a larger scale and in a more cost-effective manner to support the location needs of blind pedestrians. The local map on a smartphone interface can be used to effectively convey geometry or navigational information (such as intersection, light rail crossing, etc.) and upcoming situation (work zone, sidewalk closure, etc.) to the visually impaired in a timely manner. Its long-term impact will be determined by the usability and acceptance of the system by blind pedestrians, and by the availability and reliability of the information that is provided. To address the usability and acceptance of the assistive system, we focused our initial effort on understanding the needs and challenges of blind pedestrians at intersection crossings.

Many smartphone apps use GPS and other sensors on the phone to provide location information. However, the GPS on a smartphone doesn't work in GPS-denied environments. The benefit of our system is that it uses the BLE beacons to identify a user's location and uses a digital map of the important features as represented by the BLE beacons residing in a network to support wayfinding.

The local position and mapping information can be monitored and updated regularly from a central database system accessible to the pedestrian's smartphone. Appropriate messages can be referenced to each BLE beacon when detected by a smartphone app. The approach described here is different from all other BLE applications that have been described in the literature or public press.

The positioning and mapping method based on the BLE beacons can also be incorporated into a geospatial database or a reference map for indoor navigation and guidance. Another smartphone app

was developed for the project engineers to reduce the effort required in placing the BLE beacons at a field site. This app allows the engineers to enter the messages at the location where a Bluetooth beacon is installed. This app, for example, allows construction workers to easily reconfigure the sidewalk closure in a work zone as needed and to update the audible messages in a timely manner.

Although, our application was initially designed for people with vision impairment. The design can also benefit all users who require additional navigation information in an unfamiliar environment.

6.2 SYSTEM LIMITATIONS

Our system is intended to use the smartphone as a personal assistive device to provide transportation information to people with vision impairment. However, it does not account for the differences in personal understanding and perception of an environment. Possible system limitations include: (1) when using the smartphone as a pointer to survey the environment for geometry information, users may not point the phone in the same direction as they are facing; (2) the user's cognitive understanding of the environment and provided messages may vary; and (3) an offset of 3.5 meters in any direction is still quite a range for positioning oneself with potentially hazard tasks. We believe, the advent of even better technologies related to position localization, Location Based Services (LBS), advanced traffic signal controllers, and wireless technologies will enhance the performance and reliability of the proposed system. These issues will need to be investigated and further improved in future studies.

REFERENCES

Aira Tech Corp. (2018). https://aira.io/ retrieved October 2018.

Almaula, V., & Cheng, D. (2006). *Bluetooth Triangulator*, (Tech. rep.). San Diego: Department of Computer Science and Engineering, University of California. https://cseweb.ucsd.edu/classes/fa06/cse237a/finalproj/almula.pdf, retrieved October 2018.

Altini, M., Brunelli, D., Farella, E., & Benini, L., (2010). Bluetooth indoor localization with multiple neural networks, *2010 5th IEEE International Symposium on Wireless Pervasive Computing (ISWPC),* p. 295-300, Modena, Italy, May 5-7, 2010. https://ieeexplore.ieee.org/stamp/stamp.jsp?arnumber=5483748, retrieved October 2018.

Bandara, U., Hasegawa, M., Inoue, M., Morikawa, H., & Aoyama, T., (2004). Design and Implementation of a Bluetooth Signal Strength Based Location Sensing System, *IEEE Radio and Wireless Conference*, p.319-322, Atlanta, GA, Sep. 19-24, 2004. https://ieeexplore.ieee.org/document/1389140/, retrieved October 2018.

Barbeau, S.J., Georggi, N.L., & Winters, P.L. (2010). Integration of GPS-Enabled Mobile Phones and AVL: Personalized Real-Time Transit Navigation Information on Your Phone, *Proceedings of the National Academy of Sciences, Transportation Research Board 89th Annual Meeting*, Washington, D.C.

Barlow, J.M., Bentzen, B.L., & Bond, T. (2005). Blind Pedestrians and the Changing Technology and Geometry of Signalized Intersections: Safety, Orientation, and Independence. J. of Visual Impairment & Blindness, 99(10), 587–598.

Bekiaris, E., Kalogirou, K. & Panou, M. (2007), Personalised infomobility services within ASK-IT project. *Proceedings of the 14th ITS World Congress*, Beijing, China, Oct. 9-13, 2007.

Bentzen, B.L., Barlow, J.M. & Franck, L. (2002). *Determining Recommended Language for Speech Messages used by Accessible Pedestrian Signals*. Final Report. Berlin, MA: Accessible Design for the Blind.

Bluetooth SIG. (2018). What is Bluetooth Technology, https://www.bluetooth.com/, retrieved October 2018.

Bohonos, S., Lee, A., Malik, A., Thai, C., & Manduchi, R. (2008). *Cellphone Accessible Information via Bluetooth Beaconing for the Visually Impaired.* Santa Cruz: University of California, Santa Cruz, CA. http://citeseerx.ist.psu.edu/viewdoc/download?doi=10.1.1.153.4591&rep=rep1&type=pdf, retrieved October 2018.

Bourquin, E., Wall Emerson, R., Sauerburger, D., & Barlow, J. (2018). Conditions that influence drivers' behavior at a roundabout: Increasing yielding for pedestrians who are visually impaired. *Journal of Visual Impairment & Blindness*, *112*(1), p.61–71.

Bourquin, E., Wall Emerson, R., Sauerburger, D., & Barlow, J. (2017). The Effect of the Color of a Long Cane Used by Individuals Who Are Visually Impaired on the Yielding Behavior of Drivers. *Journal of Visual Impairment & Blindness*, *111*(5), p.401–410.

Bourquin, E., Wall Emerson, R., Sauerburger, D., & Barlow, J. (2016). Conditions that influence drivers' yielding behavior: Effects of pedestrian gaze and head movements. *International Journal or Orientation and Mobility*, *8*(1), p.13–26.

Bourquin, E., Wall Emerson, R., Sauerburger, D., & Barlow, J. (2014). Conditions that Influence Drivers' Yielding Behavior in Turning Vehicles at Intersections with Traffic Signal Controls. *Journal of Visual Impairment & Blindness*. Retrieved from http://www.afb.org/store/Pages/ShoppingCart/ProductDetails.aspx?ProductId=jvib080302&ruling=No, October 2018.

Bourquin, E., Wall Emerson, R., & Sauerburger, D. (2011). Conditions that Influence Drivers' Yielding Behavior for Uncontrolled Intersections. *Journal of Visual Impairment & Blindness, 105*(11), 760–769.

Brown, R.G., & Hwang, P.Y.C., (2012) *Introduction to Random Signals and Applied Kalman Filtering*, 4th ed. Hoboken, NJ: John Wiley.

Castaño, J.G., Svensson, M., and Ekström, M., (2004). Local Positioning for Wireless Sensors Based on Bluetooth, *IEEE Radio and Wireless Conference,* p.195-198, Atlanta, GA, Sep. 19-22, 2004. https://ieeexplore.ieee.org/document/1389106/, retrieved October 2018.

Chen, Y., Pan, Q., Liang, Y., & Hu, Z. (2010) AWCL: Adaptive weighted centroid target localization algorithm based on RSSI in WSN, *3rd International Conference on Computer Science and Information Technology*, p. 331-336, Chengdu, China, July 9-11, 2010. https://ieeexplore.ieee.org/document/5565022/, retrieved October 2018.

Chen Z., Zhu, Q., & Soh Y.C. (2016). Smartphone Inertial Sensor-Based Indoor Localization and Tracking with iBeacon Corrections. *IEEE Transactions on Industrial Informatics*, *12*(4), p. 1540–1549.

Coldefy, J. (2009). The Mobiville Project: Large Scale Experimentation of Real-Time Public Transport Information Service Providing Satellite Based Pedestrian Guidance on Smart Phones. *Proceedings of the 16th ITS World Congress, Stockholm*, Sweden, Sep. 21-25, 2009.

Davidson P. & Piché, R. (2017) A Survey of Selected Indoor Positioning Methods for Smartphones, *IEEE Communications Surveys & Tutorials*, *19*(2), p. 1347–1370.

Dawidson, E. (2009). Pedestrian Navigation in Stockholm, How Local Data Together with Advanced Positioning Techniques Can Be Used for Detailed Routing. *Proceedings of the 16th ITS World Congress*, Stockholm, Sweden, Sep. 21-25, 2009.

Diaz, J.J.M., Maues, R. de A., Soares, R.B., Nakamura, E.F., & Figueiredo, C.M. S. (2010). Bluepass: An indoor Bluetooth-based localization system for mobile applications, 2010 IEEE Symposium on Computers and Communications (ISCC), p.778-783, Riccione, Italy, Jun. 22-25, 2010.

Dong, Q., & Dargie, W., (2012). Evaluation of the reliability of RSSI for indoor localization, *Wireless Communications in Unusual and Confined Areas (ICWCUCA), 2012 International Conference*, p.1-6, Clermont-Ferrand, France, Aug. 28-30, 2012.

Edwards, S., Bryan, H., & Wagner, J. (2007). Indoor Localization for Disabled People: ASK-IT Project, *Proceedings of the 14th ITS World Congress*, Beijing, China, Oct. 9-13, 2007.

Empco-Lite. (2018). http://www.empco-lite.com, retrieved October 2018.

Faheem, A., Virrankoski, R., & Elmusrati, M. (2010). Improving RSSI Based Distance Estimation for 802.15.4 Wireless Sensor Networks, *IEEE International Conference on Wireless Information Technology and Systems (ICWITS)*, p.1-4, Honolulu, HI, Aug. 28-Sep. 3, 2010.

Fan, S.-H., Hsu, Y.-T., & Sung, F.-Y., (2015). An Enhanced Device Localization Approach Using Mutual Signal Strength in Cellular Networks, *IEEE Internet of Things Journal*, *2*(6), pp. 596–603.

Fan, S.-H., & Lin, T.-N., (2008). Robust Wireless LAN Location Fingerprinting by SVD-based noise reduction, *Proc. Communication Control Signal Processing, ISCCSP 3rd International Symposium*, p. 295-298, St Julians, Malta, Mar. 12-14, 2008.

Faragher, R., & Harle, R., (2014) An Analysis of the Accuracy of Bluetooth Low Energy for Indoor Positioning Applications, *Proceedings of the 27th International Technical Meeting of The Satellite Division of the Institute of Navigation (ION GNSS*), p. 201-210, Tampa, FL, Sep. 8-12, 2014.

Fink, A., & Beikirch, H. (2011). Analysis of RSS-based location estimation techniques in fading environments, *2011 International Conference on Indoor Positioning and Indoor Navigation*, p. 1-6, Guimaraes, Portugal, Sep. 21-23, 2011.

Ganz, A., Gandhi, S.R., Schafer, J., Singh, T., Puleo, E., Mullett, G., &Wilson, C. (2011). PERCEPT: Indoor Navigation for the Blind and Visually Impaired, *33rd annual international conference of the IEEE EMBS,* p.856-859, Boston, MA, Aug. 30-Sep. 3, 2011.

Ganz, A., Schafer, J., Gandhi, S., Puleo, E., Wilson, C., & Robertson, M. (2012). PERCEPT Indoor Navigation System for the Blind and Visually Impaired: Architecture and Experimentation. *International Journal of Telemedicine and Applications*, Volume 2012, Vol.2012, Article ID 894869, p. 1-12. https://www.hindawi.com/journals/ijta/2012/894869/cta/, retrieved October 2018.

Gaunet, F. (2006). Verbal guidance rules for a localized wayfinding aid intended for blind-pedestrians in urban areas. *Universal Access in the Information Society*, *4*(4), p. 338–353.

Gaunet, F., & Briffault, X. (2005). Exploring the Functional Specifications of a Localized Wayfinding Verbal Aid for Blind Pedestrians: Simple and Structured Urban Areas. *Human Computer Interaction*, *20*(3), p. 267–314.

Giudice, N.A., Bakdash, J.Z., & Legge, G.E. (2007). Wayfinding with words: Spatial learning and navigation using dynamically-updated verbal descriptions. *Psychological Research*, *71*(3), p. 347–358.

Giudice, N. A. & Legge, G. E., (2008). Blind Navigation and the Role of Technology, In A. Helal, M. Mokhtari, & B. Abdulrazak (Eds), The *Engineering Handbook of Smart Technology for Aging, Disability, and Independence*. Hoboken, NJ: John Wiley & Sons, Inc.

Golledge, R. G. & Gärling, T. (2004). Cognitive maps and urban travel. In D. A. Hensher, K. J. Button, K. E. Haynes and P. R. Stopher (Eds), *Handbook of Transport Geography and Spatial Systems*. Amsterdam: Elsevier.

Guth, D. (2007). Why Does Training Reduce Blind Pedestrians' Veering? In J. J. Rieser, D. H. Ashmead, F. Ebner & A. L. Corn (Eds.), *Blindness and Brain Plasticity in Navigation and Object Perception* (p. 353-365): New York: Taylors & Francis Group.

Havik, E.M., Kooijman, A.C., & Steyvers, J.J.M., (2011). The Effectiveness of Verbal Information Provided by Electronic Travel Aids for Visually Impaired Persons. *Journal of Visual Impairment & Blindness, 105*(10), p. 624–637.

Hawkins, D.M., & Olwell, D.H. (1998), *Cumulative Sum Charts and Charting for Quality Improvement*, New York: Springer Verlag.

He, W., Ho, P.H., & Tapolcai, J. (2017). Beacon Deployment for Unambiguous Positioning, *IEEE Internet of Things Journal*, *4*(5), p. 1370–1379.

Hine, J., Swan, D., Scott, J., Binnie, D., & Sharp, J. (2000). Using Technology to Overcome the Tyranny of Space: Information Provision and Wayfinding. *Urban Studies*, *37*(10), p. 1757–1770.

Hossain, A.K.M.M., & Soh, W., (2007). A Comprehensive Study of Bluetooth Signal Parameters for Localization, *IEEE 18th International Symposium on Personal, Indoor and Mobile Radio Communications*, p. 1–5, Athens, Greece, Sep. 3-7, 2007.

Jeon, K.E., Tong, T., & She, J. (2016). Preliminary design for sustainable BLE Beacons powered by solar panels, *2016 IEEE Conference on Computer Communications Workshops (INFOCOM WKSHP*S), p. 103–109, San Francisco, CA, Apr. 10-15, 2016.

Johnni, P. (2009). Stockholm – A City for Everyone How New Technology Can Make Every Day Life Easier for Elderly and People with Disabilities. *Proceedings of the 16th ITS World Congress*, Stockholm, Sweden, Sep. 21-25, 2009.

Jonsson, A., Sandberg, S., & Uppgård, T., (2007). Urban guidance for the blind and visually impaired – pedestrian route planning and navigation using a mobile handset. In P. Cunningham & M. Cunningham (Eds), *Expanding the Knowledge Economy: Issues, Applications. Case Studies.* Amsterdam: IOS Press.

Jung, J., Kang, D., & Bae, C. (2013). Distance Estimation of Smart Device using Bluetooth, ICSNC 2013: *The 8th International Conference on Systems and Networks Communications*, p.13-18, Venice, Italy, Oct. 27-Nov. 1, 2013.

Kalbandhe, A.A., & Patil, S.C. (2016). Indoor Positioning System using Bluetooth Low Energy, *2016 International Conference on Computing, Analytics and Security Trends (CAST),* p. 451–455, Pune, India.

Kalman, R.E. (1960). A new approach to linear filtering and prediction problems. *Journal of Basic Engineering,* 82(1), 35–45.

Kikawa, M., Yoshikawa, T., Ohkubo, S., Takeshita, A., Shiraishi, Y., & Takahashi, O. (2010). A Presence-Detection Mehod Using RSSI of a Bluetooth Device, *International Journal of Informatics Society*, *2*(1), p. 23-31. https://lib-repos.fun.ac.jp/dspace/bitstream/ 10445/4797/2/siraisi_2010_1_ijis2_1.pdf, retrieved October 2018.

Kotanen, A., Hännikäinen, M., Leppäkoski, H., & Hämäläinen, T.D. (2003). Experiments on local positioning with Bluetooth, *IEEE, International Conference on Information Technology Computers and Communications*, p. 297–303, Las Vegas, NV, Apr. 28-30 2003.

Liao, C.-F. (2014). *Development of a Navigation System Using Smartphone and Bluetooth Technologies to Help the Visually Impaired Navigate Work Zones Safely* (Final report, MnDOT 2014-12). St. Paul, MN: Minnesota Department of Transportation.

Liao, C.-F. (2013). Using Smartphone App to Support Visually Impaired Pedestrians at Signalized Intersection Crossings, *Transportation Research Record*, *2393*, p. 12–20.

Liao, C.-F., Rakauskas, M., & Rayankula, A. (2011). *Development of Mobile Accessible Pedestrian Signals (MAPS) for Blind Pedestrians at Signalized Intersections* (Final report). Minneapolis, MN: Univeristy of Minnesota, Intelligent Transportation Systems (ITS) Institute (CTS 1-11).

Liao, C.-F., Fan, Y., Adomavicius, G., & Wolfson, J. (2016). Battery-Efficient Location Change Detection for Smartphone-Based Travel Data Collection: A Wi-Fi Fingerprint Approach*, Compendium of 95th annual TRB meeting*, Washington, DC.

Lin, S.-Y., Liu, J.-C., & Xhao, W. (2007). Adaptive CUSUM for Anomaly Detection and its Application to Detect Shared Congestion (Technical Report: TAMU-CS-TR-2007-1-2). College Station, TX: Texas A&M University. https://engineering.tamu.edu/media/697122/tamu-cs-tr-2007-1-2.pdf, retrieved October 2018.

Liu, Y., Jin, M., & Cui, C. (2010). Modified Weighted Centroid Localization Algorithm Based on RSSI for WSN, *Chinese Journal of Sensors and Actuators, 23*, p. 716-721.

Luceño, A. (2004). CUSCORE Charts to Detect Level Shifts in Autocorrelated Noise. *International Journal Quality Technology & Quantitative Management*, *1*(1), p. 27–45.

Manual on Uniform Traffic Control Devices. (MUTCD). U.S. Department of Transportation, Federal Highway Administration, Washington D.C. https://mutcd.fhwa.dot.gov/, retrieved October 2018.

Martchouk, M., Mannering, F., & Bullock, D. (2011). Analysis of Freeway Travel Time Variability Using Bluetooth Detection. *Journal of Transportation Engineering*, *137*(10), p. 697–704.

Mautz, R. (2012). Indoor positioning technologies, 2012, Habilitation Thesis, Dept. of Civil, Environmental and Geomatic Engineering, ETH-Zürich, Zürich, Switzerland. https://doi.org/10.3929/ethz-a-007313554, retrieved October 2018.

MDI Traffic Control Products. http://www.mditrafficcontrol.com/, retrieved October 2018.

Microchip MCP73833, 1A output current linear charge management controller. http://www.microchip.com/wwwproducts/Devices.aspx?dDocName=en027785, retrieved October 2018.

Minnesota Manual on Uniform Traffic Control Devices (MN MUTCD). http://www.dot.state.mn.us/trafficeng/publ/mutcd/, retrieved October 2018.

Navarro, E., Peuker, B., & Quan, M. (2011). Wi-Fi Localization Using RSSI Fingerprinting, California Polytechnic State University. http://digitalcommons.calpoly.edu/cpesp/17/, retrieved October 2018

Oguejiofor, O.S., Okorogu, V.N., Adewale, A., & Osuesu, B.O. (2013). Outdoor Localization System Using RSSI Measurement of Wireless Sensor Network*, International Journal of Innovative Technology and Exploring Engineering* (*IJITEE), 2*(2), p. 1–6.

Oliveira, T., Raju, M., & Agrawal, D., (2012). Accurate Distance Estimation Using Fuzzy Based Combined RSSI/LQI Values in an Indoor Scenario: Experiment Verification, *Network Protocols and Algorithms*, *4*(4), p. 174–199.

Ozer A., & John, E. (2016). Improving the Accuracy of Bluetooth Low Energy Indoor Positioning System Using Kalman Filtering*, 2016 International Conference on Computational Science and Computational Intelligence (CSCI),* p. 180-185, Las Vegas, NV, Dec. 15-17, 2016. https://ieeexplore.ieee.org/document/7881334/, retrieved October 2018.

Palumbo, F., Barsocchi, P., Chessa, S., & Augusto, J.C. (2015). A stigmergic approach to indoor localization using Bluetooth Low Energy beacons, *2015 12th IEEE International Conference on Advanced Video and Signal Based Surveillance (AVSS)*, Karlsruhe, pp. 1-6.

Pei, L., Chen, R., Liu, J., Kuusniemi, H., Tenhunen, T., & Chen, Y. (2010). Using Inquiry-based Bluetooth RSSI Probability Distributions for Indoor Positioning, *Journal of Global Positioning Systems*, *9*(2), p. 122-130.

Ponchillia, P., Rak, E., Freeland, A., & LaGrow, S. (2007). Accessible GPS: Reorientation and Target Location Among Users with Visual Impairments. *Journal of Visual Impairment & Blindness*, *101*(7), 389–401.

Raghavan, A.N., Ananthapadmanaban, H., Sivamurugan, M.S., Ravindran, B. (2010). Accurate mobile robot localization in indoor environments using Bluetooth. *Robotics and Automation (ICRA), 2010 IEEE International Conference*, p.4391–4396, Anchorage, Alaska, May 3-8, 2010. https://ieeexplore.ieee.org/document/5509232/, retrieved October 2018.

Rajaraman, A., & Ullman, J.D. (2011). *Mining of Massive Datasets*: Chapter 3. New York: Cambridge University Press.

Rida, M.E., Liu, F., Jadi, Y., Algawhari, A.A.A., & Askourih, A. (2015) Indoor Location Position Based on Bluetooth Signal Strength, *2015 2nd International Conference on Information Science and Control Engineering,* p. 769–773, Shanghai, China, Apr. 24-26, 2015. https://ieeexplore.ieee.org/document/7120717/, retrieved October 2018.

Roos, T., Myllymaki, P., Tirri, H., Misikangas, P., & Sievanen, J. (2002). A probabilistic approach to WLAN user location estimation*, International Journal of Wireless Information Networks*, *9(*3), p. 155–164.

Sagias, C., & Karagiannidis, K. (2005). Gaussian class multivariate Weibull distributions: theory and applications in fading channels, *IEEE Transactions on Information Theory*, *51*(10), p. 3608–3619.

Sheng, Z., & Pollard, J. K. (2006). Position Measurement Using Bluetooth, *IEEE Transactions on Consumer Electronics*, *52*(2), p. 555–558.

Shi, H. (2012). A new weighted centroid localization algorithm based on RSSI, *2012 IEEE International Conference on Information and Automation*, p. 137-141, Shenyang, China, Jun. 6-8, 2012. https://ieeexplore.ieee.org/document/6246797/, retrieved October 2018.

Spachos, P., & Mackey, A. (2018). Energy efficiency and accuracy of solar powered BLE beacons. *Computer Communications*, *119*, p. 94–100.

Suárez, A., Elbatsh, K.A., & Macías, E. (2010). Gradient RSSI Filter and Predictor for Wireless Network Algorithms and Protocols. *Network Protocols and Algorithms*, *2*(2), 1–26.

Subhan, F., Hasbullah, H., Rozyyev, A., & Bakhsh, S.T., (2011). Indoor positioning in Bluetooth networks using fingerprinting and lateration approach, *Information Science and Applications (ICISA), 2011 International Conference*, p.1–9, Jeju Island, Republic of Korea, April 26-29, 2011.

Subhan, F., Hasbullah, H., & Ashraf, K., (2013) Kalman Filter-Based Hybrid Indoor Position Estimation Technique in Bluetooth Networks. *International Journal of Navigation and Observation*, *(2013),* p. 13.

Subhan, F., Ahmed, S., Ashraf, K., & Imran, M., (2015). Extended Gradient RSSI Predictor and Filter for Signal Prediction and Filtering in Communication Holes. *Wireless Personal Communications*, *83*(1), p. 297–314

The ASK-IT project. (2009). http://www.ask-it.org/, retrieved October 2018.

The e-Adept accessibility project. (2009). http://www.eadept.se, retrieved October 2018.

The NOPPA project. (2009). http://virtual.vtt.fi/virtual/noppa/noppaeng.htm, retrieved October 2018.

Ullman, B.R., & Trout, N.D. (2009). Accommodating Pedestrians with Visual Impairments In and Around Work Zones. *Journal of the Transportation Research Board*, *2140*(-1), 96–102.

Virtanen A. & Koshinen. S. (2004). NOPPA – Navigation and Guidance System for the Blind. *Proceedings of the 11th ITS World Congress*, Nagoya, Japan, Oct. 18-24, 2004.

Wang, Y., Shi, S., Yang, X., & Ma, A., (2010). Bluetooth Indoor Positioning using RSSI and Least Square Estimation, *2010 2nd International Conference on Future Computer and Communication (ICFCC),* Shanghai, China, May 21-24, 2010.

Wang, Y., Yang, X., Zhao, Y., Liu, Y., & Cuthbert, L. (2013). Bluetooth positioning using RSSI and triangulation methods, *2013 IEEE Consumer Communications and Networking Conference (CCNC),* p. 837–842, Las Vegas, NV. http://ieeexplore.ieee.org/stamp/stamp.jsp?tp=&arnumber=6488558, retrieved October 2018.

Wilson, J., Walker, B. N., Lindsay, J., Cambias, C., & Dellaert, F., (2007). SWAN: System for Wearable Audio Navigation. *Proceedings of the 11th International Symposium on Wearable Computers*, Boston, MA, p. 91–98, Oct. 11-13, 2007. https://ieeexplore.ieee.org/document/4373786/, retrieved October 2018.

Yoon, P.K., Zihajehzadeh, S., Kang, B.S., & Park, E.J. (2015). Adaptive Kalman filter for indoor localization using Bluetooth Low Energy and inertial measurement unit, *2015 37th Annual International Conference of the IEEE Engineering in Medicine and Biology Society (EMBC)*, Milan, Italy, p. 825–828. Aug. 25-29, 2015. https://ieeexplore.ieee.org/document/7318489/, retrieved October 2018.

Youssef, M.A., Agrawala, A., & Udaya Shankar, A. (2003). WLAN location determination via clustering and probability distributions, *Proceedings of the 1st IEEE International Conference on Pervasive Computing and Communications*, p. 143–150. Fort Worth, TX, Mar. 26, 2003. https://ieeexplore.ieee.org/document/1192736/, retrieved October 2018.

Zhang, L., Liu, X., Song, J., Gurrin, C., & Zhu, Z. (2013). A Comprehensive Study of Bluetooth Fingerprinting-Based Algorithms for Localization, *IEEE 27th International Conference on Advanced Information Networking and Applications Workshops (AINA),* p. 300–305, Barcelona, Spain, Mar. 23-28, 2013. http://ieeexplore.ieee.org/stamp/stamp.jsp?tp=&arnumber=6550414, retrieved October 2018.

Zhao, F., Zhao, Q. & Chen, H. (2011). TDOA localization algorithm based on RSSI weighted data fusion. *Journal of Guilin University of Electronic Technology, 31*(4), p. 275-279.

Zhu, J., Chen, Z., Luo, H., & Li, Z., (2014). RSSI Based Bluetooth Low Energy Indoor Positioning, *2014 International Conference on Indoor Positioning and Indoor Navigation*, p.526-533, Busan, Korea, Oct. 27-30, 2014. https://ieeexplore.ieee.org/document/7275525/, retrieved October 2018.

Zhuang, Y., Yang, J., Li, Y., Qi, L., & El-Sheimy, N. (2016). Smartphone-based indoor localization with Bluetooth low energy beacons. *Sensors, 16*(5), 596.

APPENDIX A
MATRIC DIFFERENTIATION

A.1 Proposition #1

Let's define a scalar α as,

$$\alpha = Y^T AX \tag{A-1}$$

Where,

Y is an m × 1 vector,

X is an n × 1 vector,

A is an m × n, and A is independent of X and Y.

Then,

$$\frac{\partial \alpha}{\partial X} = Y^T A \tag{A-2}$$

And,

$$\alpha = \alpha^T = X^T A^T Y \tag{A-3}$$

Therefore,

$$\frac{\partial \alpha}{\partial Y} = X^T A^T \tag{A-3}$$

A.2 Proposition #2

For a special case in which the scalar α is defined as,

$$\alpha = X^T AX \tag{A-4}$$

Where,

X is an n × 1 vector,

A is an n × n, and A is independent of X.

Then,

$$\frac{\partial \alpha}{\partial X} = X^T A + X^T A^T = X^T (A + A^T) \tag{A-5}$$

When A is a symmetric matrix, then

$$\frac{\partial \alpha}{\partial X} = 2X^T A \tag{A-6}$$

APPENDIX B

DRAWINGS OF SOLAR PANEL MOUNTING ASSEMBLY

Figure B.1 is the drawings for two 1-in angle bars that were directly attached to the solar panel. Another two ¾ in angle aluminum bars (as illustrated in Figure B.2) were used for adjusting the tilt angle of the solar panel. And, the mounting L bracket shown in Figure B.3 was used for attaching the entire assemble to a lamp post using a stainless steel worm gear clamp (Figure B.4).

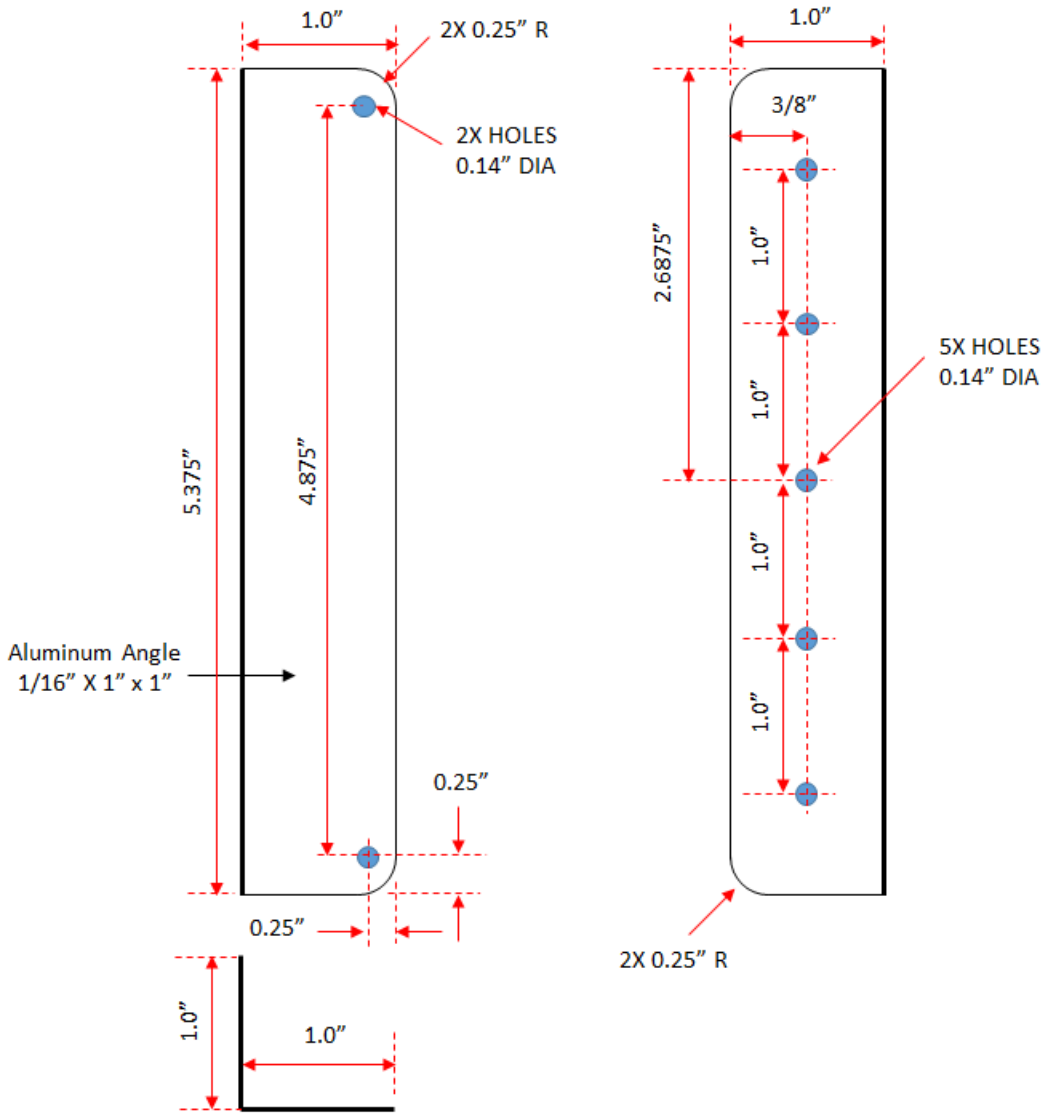

Figure B.1 Drawings of Angle Bar for Holding Solar Panel

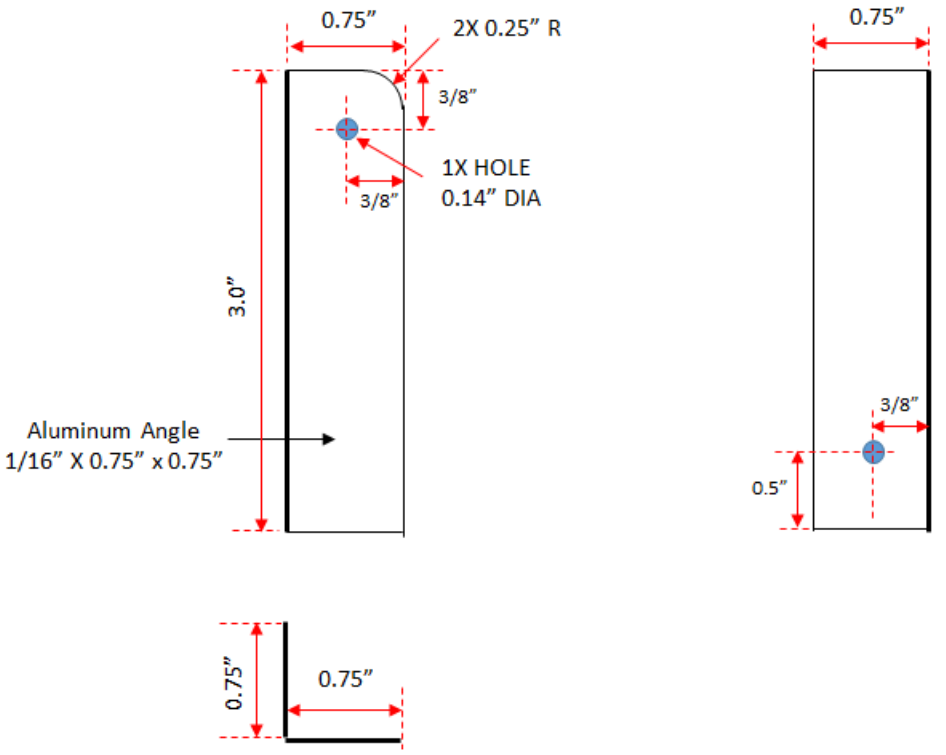

Figure B.2 Angle Bars for Tilt Angle Adjustment

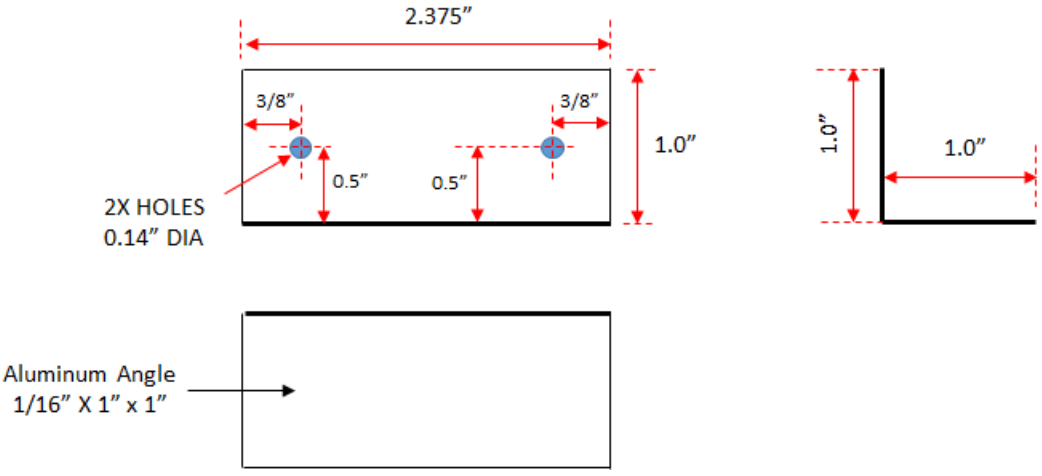

Figure B.3 Mounting L-Bracket

Figure B.4 Solar Panel Mounting Assembly